Journal of Neuroscience Methods 360 (2021) 109269

Contents lists available at ScienceDirect

Journal of Neuroscience Methods

journal homepage: www.elsevier.com/locate/jneumeth

The role of electroencephalography electrical reference in the assessment of functional brain–heart interplay: From methodology to user guidelines

Diego Candia-Rivera [*,1], Vincenzo Catrambone [2], Gaetano Valenza [3]

Bioengineering and Robotics Research Center E. Piaggio and the Department of Information Engineering, School of Engineering, University of Pisa, Pisa, Italy

ARTICLE INFO

Keywords:
Brain-heart interplay
EEG reference
Heart rate variability
Heartbeat evoked responses

ABSTRACT

Background: The choice of EEG reference has been widely studied. However, the choice of the most appropriate re-referencing for EEG data is still debated. Moreover, the role of EEG reference in the estimation of functional Brain-Heart Interplay (BHI), together with different multivariate modelling strategies, has not been investigated yet.

Methods: This study identifies the best methodology combining a proper EEG electrical reference and signal processing methods for an effective functional BHI assessment. The effects of the EEG reference among common average, mastoids average, Laplacian reference, Cz reference, and the reference electrode standardization technique (REST) were explored throughout different BHI methods including synthetic data generation (SDG) model, heartbeat-evoked potentials, heartbeat-evoked oscillations, and maximal information coefficient.

Results: The SDG model exhibited high robustness between EEG references, whereas the maximal information coefficient method exhibited a high sensitivity. The common average and REST references for EEG showed a good consistency in the between-method comparisons. Laplacian, and Cz references significantly bias a BHI measurement.

Comparison with existing methods: The use of EEG reference based on a common average outperforms on the use of other references for consistency in estimating directed functional BHI. We do not recommend the use of EEG references based on analytical derivations as the experimental conditions may not meet the requirements of their optimal estimation, particularly in clinical settings.

Conclusion: The use of a common average for EEG electrical reference is concluded to be the most appropriate choice for a quantitative, functional BHI assessment.

1. Introduction

The advantages of electroencephalography (EEG) for measuring scalp brain activity, i.e., high time resolution or non-invasiveness, have allowed it to be used as a reference tool for clinical studies and cognitive neuroscience research. The critical role of the electrical reference in the evaluation of neural activity through spontaneous brain responses or event-related potentials was explained in a previous study (Hagemann et al., 2001). Indeed, EEG recordings require a physical reference to measure the differences in electrical potentials. However, the measurement of potentials at the selected reference electrode may capture some ongoing neural activity, which may contaminate the overall measurement (Lehmann, 1984). Moreover, the computation of EEG markers, i.e., indices computed from EEG data to describe the underlying physiological phenomena, may be affected by the specific EEG reference (Hagemann et al., 2001). These EEG reference issues have been widely studied, with researchers advocating for the necessity of offline re-referencing of data to overcome the problem (Miller et al., 1991; Hagemann et al., 2001; Kayser and Tenke, 2010; Hu et al., 2018). Although there is a general consensus in the scientific community on the necessity of EEG re-referencing, the choice of the most appropriate method is still debated (Desmedt et al., 1990; Pascual-Marqui and Lehmann, 1993). Most state-of-the-art EEG reference studies have arrived at the conclusion that the best EEG reference is different for

* Corresponding author.
E-mail address: diego.candia.r@ug.uchile.cl (D. Candia-Rivera).
[1] ORCID: 0000-0002-4043-217X
[2] ORCID: 0000-0001-9030-7601.
[3] ORCID: 0000-0001-6574-1879.

https://doi.org/10.1016/j.jneumeth.2021.109269
Received 23 September 2020; Received in revised form 16 June 2021; Accepted 18 June 2021
Available online 24 June 2021

different experimental paradigms and the underlying neural sources (Dien, 1998; Kayser and Tenke, 2010).

In this study, we demonstrate that it is necessary to properly define the methodological standards of an EEG reference for existing markers made for functional brain-heart interplay (BHI) assessment. In fact, the role of the EEG reference in the estimation of BHI markers has not been investigated thoroughly yet, and preliminary studies were only recently published (Candia-Rivera et al., 2020a, 2020b). The effects of changing the EEG reference could be translated into several distortions, including temporal dynamics disparities or even power spectrum variations (Yao et al., 2005; Lei and Liao, 2017). These distortions may lead to inaccurate BHI assessment, affecting specifically the measurement of event-related evoked activity or tonic oscillatory activity in specific frequency bands. Moreover, an improper EEG reference may mislead to topographical changes among scalp electrodes that may not be related to actual spatial differences in directional functional BHI.

To avoid these issues, in this study we investigate different BHI methods together with specific EEG references. In fact, it is expected that the level of sensitivity would change depending on the underlying computation strategies used to assess the functional BHI. Some BHI methods rely on specific cardiac-event-related amplitudes in either the time domain or the frequency domain (Schandry et al., 1986; Grosselin et al., 2018), while others rely on the level of agreement with parallel cardiac oscillations (Valenza et al., 2016a; Catrambone et al., 2019b). Next, we review the most used EEG references over four methods for assessing functional BHI. The experimental results were gathered from two different dataset: the first comprises data from 28 healthy subjects in resting state, and the second publicly available dataset comprises data from up to 23 healthy subjects undergoing emotional video elicitation (Soleymani et al., 2012).

1.1. The role of electrical reference on EEG

Proper measurement of cortical potentials, through studies on brain dynamics using EEG and event-related potentials, has led to the development of several methods for the EEG reference (Miller et al., 1991). The methods range from such simple solutions as using individual or a combination of electrodes located either within or outside the scalp electrodes to more complex methods that use analytical estimations to derive the actual scalp potentials. In this study, we present an overview on five common methods (Hagemann et al., 2001; Kayser and Tenke, 2010).

Uni-polar references have been vastly employed in the past, with midline electrodes such as Fz, Cz, Pz or Oz being used (Lehmann, 1984). One of the most used methodologies is the vertex reference (CZ), which is usually employed as the physical reference in EEG recordings. One issue reported for unipolar references is related to possible distortions in within-electrodes measurements, such as connectivity, correlations, phase synchrony, or coherence, depending on the relative amplitude or power with respect to the signal recorded from the reference electrode (Hu et al., 2010). The main questioning of using the CZ reference stems from the computation of potential difference with respect to an active cortical area (Lehmann, 1984; Hagemann et al., 1998).

Another strategy involves selecting electrodes outside the scalp that might not capture neural activity, such as body parts (Wolpaw and Wood, 1982; Hu et al., 2012) or mastoids (Stephenson and Gibbs, 1951). In this study, we explored the mastoids average reference (MA), which, in a previous study, was associated with a reduced neural activity area with respect to cephalic sites (Hagemann et al., 1998). However, previous studies demonstrated a reduced robustness to changes in the EEG montage of the MA reference, when compared with other EEG references (Hu et al., 2018). The MA reference also presented challenges when evaluating connectivity (Qin et al., 2010) or event-related potentials in adjacent regions (Kayser et al., 2007). The reference electrode may cause distortions in nearby regions due to the electromagnetic field it generates (Miller et al., 1991).

The common average reference (AV) is a common method used in EEG studies (Dien, 1998; Picton et al., 2000). The AV reference corresponds to the potentials measured in the EEG dataset averaged across the whole scalp or a subset of channels (Offner, 1950; Bertrand et al., 1985). Earlier studies have proposed the AV reference given its independence to specific scalp regions (Kayser and Tenke, 2010), besides possessing other advantages such as the robustness to changes in experimental conditions (Bertrand et al., 1985). Nevertheless, it still has a few disadvantages, e.g., its performance varies with the number of EEG electrodes used in the experimental setup, and with the criterion of selection of the electrode subset in high-density EEG systems (Bertrand et al., 1985; Junghöfer et al., 1999). The spectral analysis might also get affected by the influence of the electrodes' average power on the EEG measurement. (Fein et al., 1988).

In response to the distortions produced by EEG channels when directly used as reference, researchers have proposed analytical methods as the Laplacian reference (LP) (Nunez, 1989). This method considers the current sources captured in space dimensions. It considers the changes in current density across the scalp with respect to the brain's electrical field curvature and models the head as a concentric sphere. The LP reference has been mainly tested on scalp potentials, and its advantage in detecting smaller potentials generated from localised sources has been reported (Nunez, 1989; He et al., 2001). Even though it is an analytical method, the LP reference is not exempt from the effects of the number of EEG electrodes, as mentioned for the AV reference as well (Nunez et al., 1994). Other issues with the use of LP reference that have been reported include variation of performance with respect to the frequency bands studied (Srinivasan et al., 1998) or with the electrode location used (Carvalhaes and de Barros, 2015). The main limitation of this method is that it was mostly designed and tested for high-density EEG systems (He et al., 2001; Kayser and Tenke, 2015).

The reference electrode standardisation technique or REST (RS) attempts to standardize the EEG to a point tending to infinity (Yao, 2001). Despite being a more recent development, this method has been tested for various experimental setups as well as in different frequency-related studies (Yao et al., 2005; Marzetti et al., 2007) and default network analysis (Qin et al., 2010). Most importantly, this method considers the temporal dynamics of waves from EEG recordings (Yao, 2001), demonstrating its robustness to various EEG setups with different channel numbers (Hu et al., 2018). Nevertheless, this method is sensitive to added noise, compared with AV reference, and therefore not recommended for use with noisy experimental setups (Hu et al., 2018).

1.2. Functional brain–heart interplay assessment

The brain communicates with peripheral organs through processes of sensing, integration, and regulation of bodily activity (Chen et al., 2021; Quigley et al., 2021). Indeed, the heart continuously relays on the cerebral cortex in specific structures in order to perform cardiac monitoring and maintain neural homeostasis (Critchley and Harrison, 2013). The central autonomic network has been defined as a complex of brain regions and connections, controlling autonomic regulation in a variety of physiological conditions (Thayer and Lane, 2009; Silvani et al., 2016; Valenza et al., 2019, 2020). This network spans from high order regions, i.e., medial prefrontal cortex and insula, to the forebrain, i.e., hypothalamus and amygdala, and several nuclei in the medulla, e.g., nucleus of tractus solitarius, nucleus ambiguous, parabrachial Kolliker fuse nucleus (Silvani et al., 2016; Valenza et al., 2020).

The neural processing of cardiac activity has been studied from heartbeat-related scalp potentials (Schandry et al., 1986), as well as heartbeat-evoked changes in specific EEG frequency bands (Grosselin et al., 2018; Kim and Jeong, 2019). Over the past few years, abundant clinical evidence has been gathered showing a correlation between brain conditions and cardiac outputs in terms of diagnoses and outcomes. This correlation indicates that cardiac-based markers may reveal the overall mental-health state of a patient (Esler, 1998; Craig, 2003; Thayer et al.,

2012; Beissner et al., 2013; Silvani et al., 2016). Moreover, research has shown that autonomic activity is altered by such conditions as brain damage (Tahsili-Fahadan and Geocadin, 2017; Candia-Rivera et al., 2021a), insomnia (Jiang et al., 2015), epilepsy (Calandra-Buonaura et al., 2012), Parkinson's disease (Valenza et al., 2016c), anxiety (Sanchez-Gonzalez et al., 2015) and depression (Valenza et al., 2014a, 2015, 2016b).

In the other functional direction, clinical trials have characterised bidirectional brain–heart interactions during sleep (Faes et al., 2014; Lechinger et al., 2015; Perogamvros et al., 2019), and reported that external cardiac modulations could improve outcomes in patients with depression (Karavidas et al., 2007; Martin and Martín-Sánchez, 2012), and the contribution of the heart in the evaluation of consciousness after brain damage (Raimondo et al., 2017; Candia-Rivera et al., 2021a). Besides, selfhood and bodily states have been associated with aspects involving emotions, attention and subjectivity in healthy subjects (Damasio, 1999; Park and Tallon-Baudry, 2014; Blanke et al., 2015; Tallon-Baudry et al., 2018; Candia-Rivera et al., 2021b). Although there is no scientific consensus on the mechanisms involved in emotions and bodily states (Craig, 2002, 2009; Damasio, 2010; Pace-Schott et al., 2019), there is plenty of evidence suggesting that fluctuating mood and emotion elicitation involve autonomic responses that affect cardiovascular dynamics (Taggart et al., 2011; Valenza et al., 2014b). More recently, the parallel observation of EEG dynamics and instantaneous heart rate changes have revealed a relationship between emotions processing and the brain–heart axis (Valenza et al., 2016a; Catrambone et al., 2019a; Candia-Rivera et al., 2021b). Initial observations of heartbeat-related scalp potentials were related to the neural processing of cardiac activity and interoceptive awareness (Montoya et al., 1993; Schandry and Montoya, 1996; Pollatos et al., 2005). Subsequently observations uncovered that the neural responses to heartbeats are related to subjective perception (Park et al., 2014; Kim et al., 2019; Al et al., 2020), preference-based decisions (Azzalini et al., 2021), and self-related cognition (Blanke et al., 2015; Babo-Rebelo et al., 2016; Park et al., 2016; Sel et al., 2017).

The central nervous system continuously interplays with the internal organs of the body. Biological signals within the body are transmitted by such mechanisms as pain and visceroreceptive and spinothalamocortical pathways (Craig, 2002). More specifically, the continuous functional interaction between the cardiac activity and brain structures including, but not limited to, the insula, anterior cingulate cortex, medial prefrontal cortex, and the amygdala has been reported (Thayer and Lane, 2009; Critchley and Harrison, 2013; Park et al., 2014, 2018; Silvani et al., 2016; Valenza et al., 2019, 2020). As heartbeats may influence the perception and processing of the external world—hence, the production of spontaneous cognition—observing neural activity while considering the cardiac oscillations may uncover certain aspects of subjectivity from a first-person perspective (Azzalini et al., 2019; Chen et al., 2021).

The understanding of these processes involving BHI may lead to relevant scientific findings and novel clinical applications, as several cardiovascular, neurological, and psychiatric disorders may be linked to BHI dysfunctions. For example, cerebrovascular accidents may be linked to ischaemic attacks with cardiac arrhythmias (Pyner, 2014), sudden cardiac death may be caused by severe brain damage (Silvani et al., 2016), and heart transplant may affect interoception, i.e. the sensing of body signals (Salamone et al., 2020). Moreover, autonomic dysfunctions may occur in the presence of stress (Taggart et al., 2011), insomnia (Jiang et al., 2015), psychosomatic disorders (Salvioli et al., 2015), depression (Penninx et al., 2013), schizophrenia, anxiety, and related mood disorders (Leistedt et al., 2011; Valenza et al., 2017). These evidences have motivated the development of BHI-related biomarkers to assess depressive conditions (Terhaar et al., 2012; Catrambone et al., 2021a), sleep disorders (Perogamvros et al., 2019), or dysfunctional emotion recognition (Salamone et al., 2021). Functional BHI measurements are also effective in detecting residual consciousness in post-comatose patients (Candia-Rivera et al., 2021a).

To this extent, several signal processing methods have been exploited for the assessment of functional BHI, and the main approaches are here summarized in Table 1. General analysis methods refer to signal processing methods that were not specifically devised for brain-heart time series but have been successfully exploited for a BHI estimation (referred as 'general' in Table 1); ad-hoc processing tools have been particularly devised for a quantitative BHI assessment (defined as 'ad-hoc' in Table 1). While the former category embeds standard signal processing techniques estimating correlation, directional coupling, co-occurrences, or phase synchronization between dynamical systems, the latter category exploits a priori knowledge or modelling specifically linked to brain and heartbeat dynamics. BHI estimation methods are further divided in three categories: physiological modelling-based approach, synchronisation measurement, and transient neural responses to heartbeats. Methods based on physiological modelling consider the brain and heartbeat oscillations within a framework of mutual influence, thus the measurement of BHI via these methods may allow a causality assessment. BHI synchronisation measurements mainly exploits information theory, whereas transient neural responses to heartbeats analyse neural activity in specific periods defined by the cardiac cycle. The functional BHI quantification methods have also been categorized with respect to the directionality assessment; for example, while Maximal Information Coefficient does not quantify a directional coupling, Heartbeat-evoked potentials provide information on the heart-to-brain direction, and Granger-causality and Synthetic data generation models account for both BHI directions. Finally, we consider the capability of estimating linear and/or nonlinear BHI and time-varying estimates in accordance with recent evidences (Samuels, 2007; Silvani et al., 2016; Catrambone et al., 2019b, 2019a). Note that neural responses to heartbeats give a time course limited to a specific time window defined by the cardiac cycle, and are usually averaged across several cardiac cycles, therefore these are considered markers with no time-varying properties.

In this study, we investigate the impact of the EEG reference in the estimation of the functional BHI, and an overview of the study workflow is shown in Fig. 1. In the frame of physiological modelling approaches, we selected the Synthetic Data Generation because it provides bidirectional and time-varying features (Catrambone et al., 2019b); in the frame of synchronisation measurements, we selected Maximal Information Coefficient as it has been tested in different BHI settings including physiological and cognitive conditions (Valenza et al., 2016a; Catrambone et al., 2019a). Finally, in the frame of transient neural responses to heartbeats we implemented the calculation of standard heartbeat-evoked potentials (Schandry and Montoya, 1996) and heartbeat-evoked oscillations (Grosselin et al., 2018).

2. Materials and methods

2.1. Dataset description

Dataset I (resting state). A group of 32 young healthy adults were recruited to participate in the study (Catrambone et al., 2019b). Data from 4 subjects were discarded due to excessive artifacts during the recordings; consequently, data from a total of 28 subjects (age range 21–41 years, median 27 years, 15 males) were retained for further analysis. Subjects were directed to rest for 4 min and the corresponding high-density 128-channels EEG with a physical electrical reference located in the vertex, and one-lead ECG were synchronously recorded through a Geodesics Polygraph input box (Electrical Geodesics, Inc.) with a 500 Hz sampling frequency.

Dataset II (emotion elicitation). We have included in our study a second dataset, recorded in a different experimental condition, and by an independent research team, as recommended for biomarkers validation studies (Woo et al., 2017). The MAHNOB-HCI dataset of emotion elicitation (Soleymani et al., 2012) comprised data gathered from healthy subjects during the visualization of 20 emotional video trials. Two trials

Table 1
State-of-the-art methods for the assessment of Brain-Heart Interplay from non-invasive recordings. The word 'descending' refers to the from-brain-to-heart direction only, as well as 'ascending' refers to the from-heart-to-brain direction only.

Approach	Method	BHI Specificity	Features	Reference
Physiological modelling	Synthetic data generation	Ad-hoc	Bi-directional, time-varying	(Catrambone et al., 2019b)
	Granger causality	General	Bi-directional, non-time-varying	(Faes et al., 2015; Greco et al., 2019)
	Point-process transfer entropy	Ad-hoc	Descending, time-varying	(Catrambone et al., 2021b)
Synchronisation measurements	Maximal information coefficient	General	Non-directional, non-time-varying	(Reshef et al., 2011; Valenza et al., 2016a)
	Joint symbolic dynamics	General	Bi-directional, non-time-varying	(Schulz et al., 2019)
	Transfer entropy	General	Bi-directional, non-time-varying	(Faes et al., 2014)
	Convergent cross-mapping	General	Bi-directional, time-varying	(Schiecke et al., 2019)
	Synchronisation likelihood	General	Non-directional, time-varying	(Dumont et al., 2004)
	Time-delay stability	General	Bi-directional, non-time-varying	(Bashan et al., 2012)
	Multifractal-MIC joint approach	General	Non-directional, non-time-varying	(Catrambone et al., 2020)
Transient neural responses to heartbeats	Heartbeat-evoked potentials	Ad-hoc	Ascending, non-time-varying	(Schandry et al., 1986; Park and Blanke, 2019)
	Heartbeat-evoked potential variance	Ad-hoc	Ascending, non-time-varying	(Candia-Rivera et al., 2021a)
	Heartbeat-evoked oscillations	Ad-hoc	Ascending, non-time-varying	(Grosselin et al., 2018)
	Heartbeat-evoked network synchronisations	Ad-hoc	Ascending, non-time-varying	(Kim and Jeong, 2019)

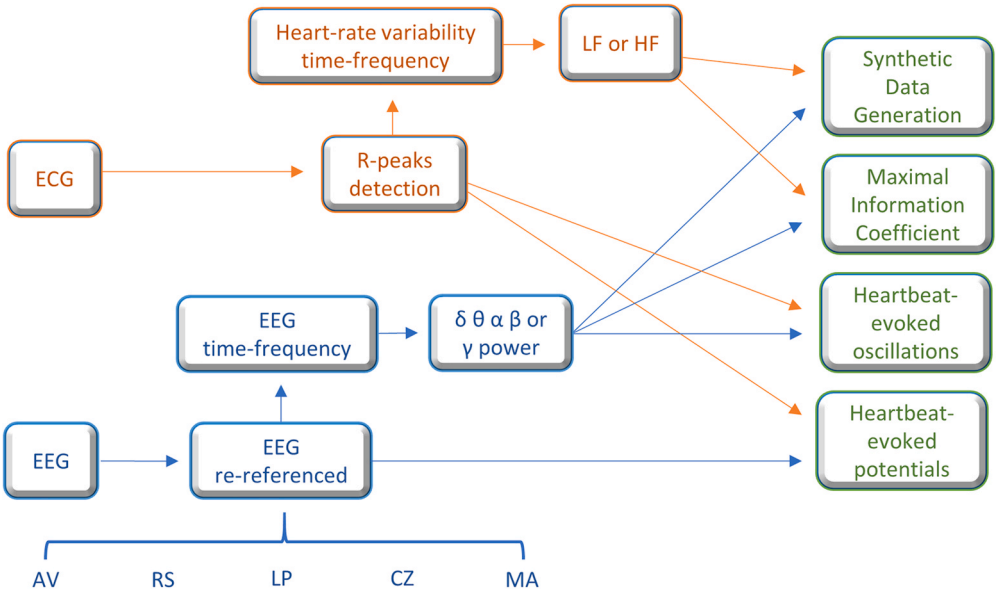

Fig. 1. Computation of functional BHI markers from the combination of two time series, one from the heart and another from the brain. Some methods use time-frequency-derived series from either one or both physiological components. In this study, the BHI markers are computed for EEG reference as AV, RS, LP, CZ, and MA.

were considered further in this study: in the first trial, labelled as "joy", data from 23 subjects were considered (age range 20–37 years, median 27 years, 11 males), whereas in the second trial, labelled as "anger", data from 21 subjects were considered (age range 20–37 years, median 27 years, 9 males). Disqualified subjects either did not give explicit consent to process their data, or physiological data were not available, or the signal quality of the ECG was not high enough to properly detect R-peaks. The selection of two trials to be included in this study relied on the circumflex model of affect (Russell, 1980), which considers a two-dimensional approach to classify emotions: valence related to pleasantness, and arousal related to emotion intensity. In this view, emotions can be determined by a linear combination of these two dimensions. The selected trials correspond to the emotions of joy and anger, which are the ones with the highest median valence and arousal from the self-assessment, respectively (Joy; median valence = 8, median arousal = 5. Anger; median valence = 1, median arousal = 7. Values in a discrete scale between 1 and 9). The "joy" video trial refers to a wedding scene from the 2003 film "Love Actually", a romantic comedy by *Richard Curtis*; and the "anger" video trial refers to an assassination scene from the 2002 film "The Pianist", a war drama by *Roman Polanski*.

2.2. EEG processing

All physiological data were pre-processed using MATLAB R2017a and Fieldtrip Toolbox (Oostenveld et al., 2011). Data were bandpass filtered with a Butterworth filter of order 4, between 0.5 and 45 Hz. EEG channels outside the scalp were not considered in this analysis (97 out of the 129 channels were considered in the resting state dataset, and all 32 channels were considered in the emotion elicitation dataset). Large movement artefacts were removed using the wavelet-enhanced

independent component analysis (Wavelet-ICA), which were identified using automated thresholding over the independent component and multiplied by ×10 to remove only very large artefacts as described in Gabard-Durnam et al. (2018). Consecutively, the ICA was re-run to recognise and reject the eye movements and cardiac-field artefacts from the EEG data (Dirlich et al., 1997). To do so, one lead from the ECG was included as an additional input in the ICA to simplify the process of finding cardiac artefacts. Once the ICA components with eye movements and cardiac artefacts were visually identified, they were set to zero to reconstruct the EEG series. The results of this step were eye-movements and cardiac-artefact-free EEG data. Thus, individual EEG channels were analysed successively. The channels were marked as contaminated if their areas under the curve exceeded 3 standard deviations (SDs) of the mean of all channels. The remaining channels were compared with their weighted-by-distance-correlation neighbours using the standard Fieldtrip neighbour's definition. If a channel resulted in a weighted-by-distance correlation of less than 0.6, it was considered contaminated. A median quantity of 5 ± 1 channels among the trials were discarded in the resting state dataset, and 2 ± 1 channels in the emotion elicitation dataset. The contaminated channels were replaced by the neighbour's interpolation as implemented on Fieldtrip. Channels were re-referenced offline using one of the methods mentioned below (see EEG reference section).

The EEG spectrogram was computed for the BHI methods requiring EEG power components. The power spectrum was computed using the short-time Fourier transform with a Hanning taper. The calculations were performed with a sliding time window of 2 s with a 50% overlap, resulting in a spectrogram resolution of 1 s and 0.5 Hz. Successively, a time series was integrated within the alpha band (8–12 Hz).

2.3. Computation of EEG electrical references

For the EEG re-reference performed in the resting state dataset, we selected 97 out of 129 channels, discarding all channels located at the face, neck and ears. Subsequently, a subset of 64 channels (out of 97 channels used until this part) were selected for the analysis, according to the 10–10 system (Luu and Ferree, 2000). The EEG re-referencing in the emotion elicitation dataset comprises all 32 channels. The references used were AV, LP, RS and CZ. The MA reference was studied in the resting state dataset only, since no mastoids electrodes were available in the MAHNOB-HCI dataset.

For computing LP reference, the Fieldtrip toolbox was used to implement the finite method (Huiskamp, 1991; Oostendorp and van Oosterom, 1996). The EEG reference is performed by estimating an EEG montage based on a constructed spatial surface grid. The electrode montage is constructed by first doing an azimuthal projection of the electrodes considering their locations in 3-dimensions, followed by a triangulation of neighbouring points of the surface grid, resulting in head modelled by a finite number of triangles. Finally, the EEG channels are referenced as mathematical combination of datapoints, based on the spatial derivatives given by the differential operator (Δ), in Eq. (1) is shown the finite estimation for electrodes with variable distances:

$$\Delta\Phi_0 = \sum_{i=1}^{N} L_i \cdot (\Phi_i - \Phi_0) \quad (1)$$

$$L_i = \frac{4}{r \cdot N} \cdot \frac{1}{r_i} \quad (2)$$

Where r is the average distance between neighbours, N is the number of neighbouring points and r_i is the triangle edge, Φ_0 the potential measured in the current point and Φ_i the potential measured in the neighbour i.

RS reference codes were downloaded from https://github.com/sccn/REST. Parameters used were 3000 default dipoles and a head model of 3 concentric spheres of thickness {0.87 0.92 1} mm, and conductivities of {1 0.0125 1} S/m for brain, skull and scalp, respectively. The computation of the RS reference is done through the measured scalp potentials and determines the electrical activity with a pipeline based on source reconstruction and a head model. In Eq. (3) is shown the RS reference representation:

$$\Phi - \Phi_{ref} = G \cdot G_{AV} \cdot R_{AV} \cdot \Phi \quad (3)$$

Where Φ is the measured potential, Φ_{ref} is the estimated EEG reference, G is the lead field, G_{AV} is the generalised Moore-Penrose inverse of demeaned G, R_{AV} is a matrix that fulfils the following expression: $\Phi_{AV} = R_{AV} \cdot \Phi$, where AV stands for Average Reference.

2.4. ECG processing

ECG data were bandpass filtered using a Butterworth filter of order 4, between 0.5 and 45 Hz. The R-peaks from the QRS waves were identified first via an automatized process, following a visual inspection of misdetections. The procedure was based on a template-based method for detecting R-peaks (Vehkaoja et al., 2013). First, 5 s were selected randomly, and the corresponding R-peaks were detected automatically by searching for the local maxima. With the detected heartbeats, an R-peak template was constructed by averaging the detected peaks at a latency of ± 0.2 s. The R-peak template was then cross-correlated with the complete ECG, and the R-peaks were detected using automated peak detection over the correlated time series. The settings of the R-peak detection method were tuned to identify peaks at a minimum distance defined by the mean inter-beat interval from the template window, adjusted by a factor of 0.8. All the detected peaks were visually inspected over the original ECG, along with the inter-beat intervals histogram. Manual corrections were performed where needed; 0–40 manual corrections were performed per subject in the resting state dataset, and 0–3 in the emotion elicitation dataset. Subjects presenting segments with unintelligible R-peaks were disqualified from the analysis, as described in datasets description section.

2.5. Heart-rate variability analysis

The heart-rate variability (HRV) series were studied in the high-frequency range (0.15–0.4 Hz) in order to quantify the parasympathetic activity from the autonomic nervous system (Acharya et al., 2006). Once the heartbeats were detected from the ECG, the HRV series were constructed as an inter-beat intervals duration time course. Consecutively, the HRV series were evenly re-sampled to 4 Hz using the spline interpolation. The HRV power was computed using a smoothed pseudo-Wigner–Ville distribution (Orini et al., 2012). The pseudo-Wigner–Ville algorithm consists of a two-dimensional Fourier transform with an ambiguity function kernel to perform two-dimensional filtering. The ambiguity function comprises ellipses whose eccentricities depend on the parameters ν_0 and τ_0, to set the filtering degrees of time and frequency domains, respectively (Costa and Boudreau-Bartels, 1995). An additional parameter λ was set to control the frequency filter roll-off and the kernel tails' size (Costa and Boudreau-Bartels, 1995; Orini et al., 2012). In this study, we set $\nu_0 = 0.03$, $\tau_0 = 0.06$ and $\lambda = 0.3$ as per previous simulation studies (Orini et al., 2012).

2.6. Computation of functional brain–heart interplay

We investigated the role of EEG reference on the main BHI assessment methods for different strategies to quantify the interplay. Synthetic Data Generation markers from the methods based on physiological modelling, Maximal Information Coefficient from the methods based on synchronisation measures, and Heartbeat-Evoked Potentials from heartbeat-locked measures and its derivative Heartbeat-Evoked Oscillations. As illustrated in Fig. 1, BHI markers were computed using a time-series component from both heart and brain. The strategies

underlying the studied BHI quantification methods vary in terms of the inputs used for its computation, as well as the outputs that provide different information in terms of time resolution and directionality of the interplay. The functional BHI was computed to obtain a single value per EEG channel, thereby the marker time course was averaged on time.

To reduce the number of confounding factors and ease the interpretation of results, we limited our investigation to time-varying EEG power series in the alpha band (8–12 Hz) and time-varying HRV power series in the HF band (0.15–0.4 Hz). This is because these features are known to characterise a resting state in healthy subjects (Acharya et al., 2006; Sadaghiani et al., 2012; Stewart et al., 2014), as well as attention level (Ray and Cole, 1985) and behavioural responses and reactivity in active tasks (Porges et al., 1994). Moreover, previous BHI studies have highlighted the interactions between EEG oscillations in the alpha band and cardiovascular oscillations in the HF band (de Munck et al., 2008; Balconi et al., 2009; Yu et al., 2009; Magosso et al., 2019).

2.6.1. Synthetic data generation (SDG)

This mathematical model assesses the bi-directional modulations between EEG oscillations at a given frequency band and heartbeat dynamics spectra integrated over low or high frequency bands (Catrambone et al., 2019b). The functional interplay going from the brain to the heart is quantified through a model able to generate synthetic heartbeat intervals based on an Integral Pulse Frequency Modulation model, which is parametrized with Poincaré Plot features (Brennan et al., 2002). The synthetic heartbeats are modelled as a summation of *Dirac* functions $\delta(t)$ in which heartbeats' timings occur at t_k. The beat-to-beat generation comprises an integration within the interbeat interval from t_k to t_{k+1}, in which the integral function reaches a threshold equal to 1, as shown in Eqs. (4) and (5), where μ_{HR} is the reference heart rate (in Hz) and $m(t)$ is the modulation function.

$$x(t) = \sum_{k=1}^{N} \delta(t - t_k) \tag{4}$$

$$1 = \int_{t_k}^{t_{k+1}} [\mu_{HR} + m(t)]dt \tag{5}$$

The modulation function $m(t)$ corresponds to the combination of two oscillators associated with cardiac oscillations in the LF and HF bands, which represent sympathovagal and parasympathetic dynamics, respectively. In Eq. (6), the amplitudes defined by C_{LF} and C_{HF} indicate the time-varying coupling constants computed parametrically from the Poincaré plot (see (Brennan et al., 2002) for further details). Therefore, the coupling coefficients $SDG_{brain\rightarrow LF}$ and $SDG_{brain\rightarrow HF}$ that represent the brain-to-heart interplay are computed as shown in Eqs. (7) and (8), where $Power_f(t-1)$ represents the EEG power time course in frequency f in the previous time window.

$$m(t) = C_{LF}(t) \cdot sin(\omega_{LF} \cdot t) + C_{HF}(t) \cdot sin(\omega_{HF} \cdot t) \tag{6}$$

$$C_{LF}(t) = SDG_{brain\rightarrow LF}(t) \cdot Power_f(t\text{-}1) \tag{7}$$

$$C_{HF}(t) = SDG_{brain\rightarrow HF}(t) \cdot Power_f(t\text{-}1) \tag{8}$$

The functional interplay from the heart to the brain is quantified through a model based on the generation of synthetic EEG series using an adaptative Markov process, in Eq. (9) (Al-Nashash et al., 2004). The model estimates the ascending modulations from the heart to the brain using least squares in an auto-regressive process, in which the Markovian neural activity generation, with a specific EEG channel, frequency band and time window, uses its previous neural activity and the current heartbeat dynamics as inputs (Eq. (10)).

$$EEG(t) = \sum_{f=f_1}^{f_n} Power_f(t) \cdot \sin(2\pi \quad f \quad t + \theta_f) \tag{9}$$

$$Power_f(t) = \kappa_f \cdot Power_f(t\text{-}1) + \Psi_f(t) + \varepsilon_f \tag{10}$$

Thereby, the coupling coefficient $SDG_{heart\rightarrow brain}$ is extracted from the estimated contribution of heartbeat dynamics HRV_X (with X as LF or HF or their combination) to the auto-regressive model for EEG data generation (Catrambone et al., 2019b):

$$SDG_{LF\rightarrow brain}(t) = \Psi_f(t) \,/\, HRV_{LF}(t) \tag{11}$$

$$SDG_{HF\rightarrow brain}(t) = \Psi_f(t) \,/\, HRV_{HF}(t) \tag{12}$$

where f is the main frequency in a defined frequency band, θ_f is the phase, κ_f is a constant and ε_f is the adjusted error. As shown in Fig. 2A, the BHI markers are obtained for the studied time course, and this allows for assessing real-time changes with a resolution defined by the power spectrum time resolution. This method was tested under sympathovagal elicitation, whereby mutual brain–heart modulations to different degrees were shown, of which the main influences observed were in the autonomic outflows toward brain dynamics involving very-low and very-high oscillations, while cortical activity between 10 and 30 Hz generally helmed part of the efferent autonomic tone (Catrambone et al., 2019b).

Source code implementing the SDG framework for functional BHI was retrieved online at https://github.com/CatramboneVincenzo/Brain-Heart-Interaction-Indexes. In this study, functional BHI measurements were derived in the direction from-the-heart-to-the-brain using time-varying EEG spectra integrated in the alpha band (8–12 Hz) and time-varying heartbeat dynamics spectra integrated in the high frequency band (0.15–0.4 Hz).

2.6.2. Maximal information coefficient (MIC)

This method quantifies linear and non-linear functional coupling between two time series (Reshef et al., 2011). The Eq. (15) shows the MIC computation using the mutual information $H(X,Y)$ between two time series X and Y. The mutual information is normalized by the minimum joint entropy, resulting in an index in the range 0–1.

$$MIC(X,Y) = \frac{H(X,Y)}{\log_2 \min\{n_X, n_Y\}} \tag{15}$$

MIC may capture non-linear correlations, which is a capability not available in traditional correlation algorithms—such as Pearson's coefficient—as it considers the similarities between two time series irrespective of signals curvatures. MIC evaluates similarities between different segments separately at an adapted time scale, as illustrated in Fig. 2B. Then, the final measure wraps the similarities across the whole time-course. The MIC has been applied to couple the time series derived from the brain and heart, obtaining one value without a time resolution. In the frame of functional BHI assessment, MIC works as a measure of brain–heart synchronisation, rather than directional modulation (Valenza et al., 2016a). As with the SDG, the MIC uses brain-oscillations time series in a specific frequency band and the heart series derived from low or high frequency range (Acharya et al., 2006). This method has been tested in emotion elicitation studies, which revealed an increase in brain–heart synchronisation under positive emotion elicitation over a wide frequency range (1–30 Hz) (Valenza et al., 2016a; Catrambone et al., 2019a).

Source code implementing MIC is available online at https://github.com/minepy. In this study, MIC was estimated between time-varying EEG spectra integrated in the alpha band (8–12 Hz) and time-varying heartbeat dynamics spectra integrated in the high frequency band (0.15–0.4 Hz).

2.6.3. Heartbeat-evoked potential (HEP)

This refers to the neural response triggered by each heartbeat (Schandry et al., 1986). It is computed using Eq. (13), which locks the N EEG epochs defined by the heartbeat time intervals and averages them

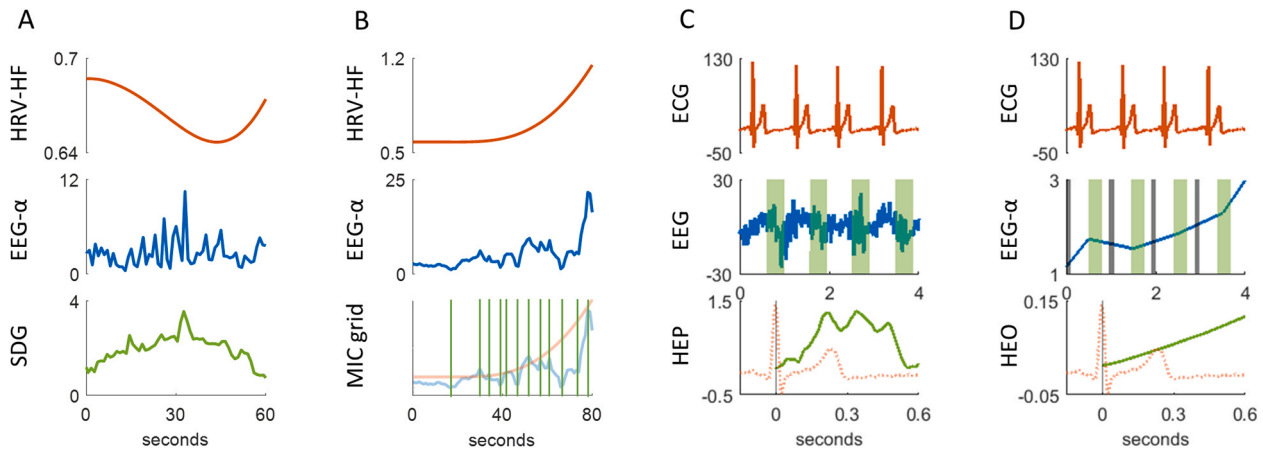

Fig. 2. Exemplary functional Brain-Heart Interplay estimates using different models. (A) SDG model (bottom panel) estimating functional coupling from the heart (HVR-HF, top panel) to the brain (EEG-α, central panel). (B) Maximal Information Coefficient (MIC) estimated between heart (HRV-HF, top panel) and brain dynamics (EEG-α, central panel), and vertical green lines in the bottom panel illustrate the grid for the MIC computation. (C) Heartbeat-evoked potential (HEP, green line in the bottom panel) computed by averaging EEG epochs (vertical green shades in the central panel) locked to R-peaks from the ECG (red lines in the top and bottom panels). (D) Heartbeat-evoked oscillations (HEO, green line in the bottom panel) computed by averaging EEG epochs in the α-band (vertical green shades in the central panel) locked to R-peaks from ECG (red lines in the top and bottom panels); EEG epochs are normalised with respect to a baseline calculated before the R-peak occurrence (vertical grey shades in the central panel). (For interpretation of the references to colour in this figure legend, the reader is referred to the web version of this article.)

to obtain the HEP, as shown in Fig. 2C.

$$\mathrm{HEP}(t) = \frac{1}{N} \sum_{k=1}^{N} \mathrm{EEG}(t,\ k) \tag{13}$$

Thus, heartbeats could be observed as brain stimulations emanating from the internal body, thereby generating a transient neural response (Azzalini et al., 2019), i.e., the HEP can be intended as a measure of BHI in the direction from-heart-to-brain. Particularly, with HEP, the neural changes can be measured with millisecond resolution. HEP features were computed by averaging the EEG epochs within the 200–500-ms interval, following each R-peak, without a baseline correction. This choice is in accordance with previous work challenging the definition of a "neutral" time window in the cardiac cycle (Park and Blanke, 2019). In order to avoid the presence of cardiac artefacts in EEG associated with the subsequent R-peak, the epoch associated with inter-beat intervals shorter than 500 ms were discarded (Park and Blanke, 2019). In this study, the HEP absolute values were considered for further analyses for consistency reasons with respect to other BHI estimation methods. HEP was computed using time-locked analysis tools from Fieldtrip toolbox, as implemented at https://github.com/diegocandiar/brain_heart_doc.

2.6.4. Heartbeat-evoked oscillations (HEO)

In the same vein, other types of heartbeat-evoked responses have been described in the domains of brain networks and brain oscillations in specific frequency bands (Grosselin et al., 2018; Kim and Jeong, 2019). In this study, we included heartbeat-evoked oscillations referring to the neural response triggered by each heartbeat within the EEG alpha band, as shown in Fig. 2D. This method has been presented to study the changes in brain oscillations with respect to cardiac or respiratory cycles (Grosselin et al., 2018). As with HEP, HEO can be considered as a quantification of the interaction between heart and brain. Eq. (14) considers the *N* power epochs referenced to a power baseline and computes the power average of a defined interval with respect to the R-peak.

$$\mathrm{HEO}_f(t) = \frac{1}{N} \sum_{k=1}^{N} [\mathrm{Power}_f(t,k)/\mathrm{Power}_{f,\mathrm{baseline}}\ (t,\ k)] \tag{14}$$

Source code implementing HEO is available online at https://github.com/FannyGrosselin/CARE-rCortex. HEO features were computed within the alpha band (8–12 Hz) by averaging EEG epochs within the 200–500 ms interval following each R-peak. The computed features account for the relative change with respect to a baseline value calculated in the −300 to −200 ms interval (i.e., before the R-peak), as recommended in (Grosselin et al., 2018).

2.7. Statistical analysis

We studied the role of the EEG reference when computing functional BHI indices. The BHI indices were computed for individual EEG channels using different electrical EEG references, i.e., AV, LP, RS, CZ and MA. We assessed the functional BHI in three different conditions: a resting state, and two emotional trials from the MAHNOB-HCI dataset (Soleymani et al., 2012). The signal processing methods employed for a BHI assessment were i) Synthetic data generation model (HRV-HF to alpha band), ii) heartbeat-evoked potentials, iii) heartbeat-evoked oscillations (alpha band), and iv) maximal information coefficient (between HRV-HF and alpha band).

Statistical analyses exploited non-parametric methods because the assumption of working with Gaussian random variables may not be verified for all samples; indeed, the Spearman correlation coefficient is bounded to the interval [−1,1] and thus cannot be associated with a Gaussian distribution. Moreover, the evaluation of rank-based differences allows for the statistical comparison between BHI assessment methods without biases due to the absolute value of the estimates; indeed, SDG, HEP, and HEO estimates are not in a normalized range [0,1] as the MIC. Accordingly, for a given variable X, group-wise descriptive statistics are expressed as Median(X) ± MAD(X), where MAD (X) = Median (|X − Median (X)|).

The following statistical analyses were performed:

I) *Comparison between EEG references*: using resting state data from Dataset I, for each EEG channel, we investigated group-wise differences between different EEG references for a given BHI assessment method through a Friedman test for paired samples; the analysis was repeated for each BHI assessment method. Moreover, using data from both Dataset I and Dataset II, for each EEG channel, we quantified pairwise similarities between different EEG references for a given BHI assessment method through Spearman correlation coefficients calculated among subjects; p-values associated with those correlation coefficients

were derived by a t-Student distribution approximation, and the analysis was repeated for each BHI assessment method.

II) *Comparison between functional BHI assessment methodologies*: using data from both Dataset I and Dataset II, for each EEG channel, we investigated group-wise differences between different BHI assessment methods for a given EEG reference through a Friedman test for paired samples; the analysis was repeated for each EEG reference.

For all statistical tests, the significance level was corrected for multiple comparisons in accordance with the Bonferroni rule considering the number of channels in each case, with a corrected statistical significance set to $\alpha = 0.05/\text{Number of channels}$.

3. Results

3.1. Comparison between EEG references in the resting state

3.1.1. Synthetic data generation model (SDG)

The results are shown in Fig. 3. The Friedman tests provided significant p-values on all electrodes on the scalp, indicating differences in SDG estimates between EEG references. Note that this result does not necessarily indicate uncorrelations between the EEG references; rather, it may indicate a significant change in the range wherein the values fluctuate. The most affected region according to the Friedman Q-stat is the vertex region (i.e, channel Cz and its neighbours). The median correlation coefficients among the channels are displayed in Table 2, with overall high correlations between SDG coefficients gathered from all EEG reference pairs (Median spearman correlation coefficient range between 0.79 and 0.98), in which the highest agreement was found between AV and RS, and the lowest between LP and MA. Despite there being high correlations between all methods, we observed that these correlations are reduced in some scalp topographies. A comparison of the LP reference with other EEG references revealed the lowest correlations between SDG coefficients, as opposed to any other EEG reference pair (Fig. 3). Conversely, the SDG coefficients computed with CZ reference have a lower correlation as compared with AV, MA, and RS in the vertex region, showing the same trend as that of the Friedman test results. Overall, the results from the SDG method indicate its robustness against the EEG reference change, given the high correlations, and the EEG reference changes cause the relative displacement of values rather than a distortion.

3.1.2. Heartbeat-evoked potentials (HEP)

The results of the Friedman test between HEP computed with different EEG references is significant for most electrodes, with higher effect size on the frontal region, as observed in Fig. 4. On the other hand, the correlations of HEP between its computations through different EEG references varies over a wide range, where the median Spearman correlation coefficients among the channels increase from 0 to 0.84, as presented in Table 3. While the highest agreement occurs between AV and RS (as seen in the SDG method), the lowest correlation is between CZ and MA. These results indicate high heterogeneity of the heartbeat-evoked potentials when changing the EEG reference. Fig. 4 presents the correlation scalp topographies for all EEG reference pairs, where region-specific changes can be observed when changing one EEG reference. The correlations including LP, namely AV–LP, LP–RS, LP–CZ and LP–MA, are low in magnitude compared with those evaluated between other EEG reference pairs. Contrarily, HEP computed with the MA reference largely agrees with the AV and RS references. Despite the high correlations, however, the AV–MA and RS–MA correlation coefficients decrease in the regions closer to the mastoids, indicating that the MA reference has a region-specific effect. The central scalp region appears to have been affected by the changing of the EEG reference, as indicated by the very low correlation of HEP as compared when computed with AV–LP, AV–CZ, LP–RS, LP–MA, RS–CZ and CZ–MA references. Indeed, the least correlated pair is CZ–MA, where the whole central region is affected. Overall, HEP presents two main affected regions—the frontal electrodes, as presented in the Friedman test, and the vertex region.

3.1.3. Heartbeat-evoked oscillations (HEO)

The Friedman test showed overall insignificant changes in the distribution for this index when changing the EEG reference, with only a small significant cluster appearing in the central-posterior region of the left hemisphere, as shown in Fig. 5. The median Spearman correlation coefficients among channels range between 0.39 and 87, as presented in Table 4. In a similar direction as other BHI methods, HEO presents the highest correlation in the AV–RS comparison. High agreements were observed also between AV–MA and RS–MA (median correlation coefficients of 0.72 and 0.73, respectively). Conversely, the effect of mastoids observed in the heartbeat-evoked potentials (Fig. 4) was not observed in this BHI index in the same manner. As indicated in Fig. 5, low correlations appear in all HEO computations with the LP reference, and the CZ–MA pair. These results indicate that heartbeat-evoked oscillations are less sensitive to EEG reference than the EEG evoked

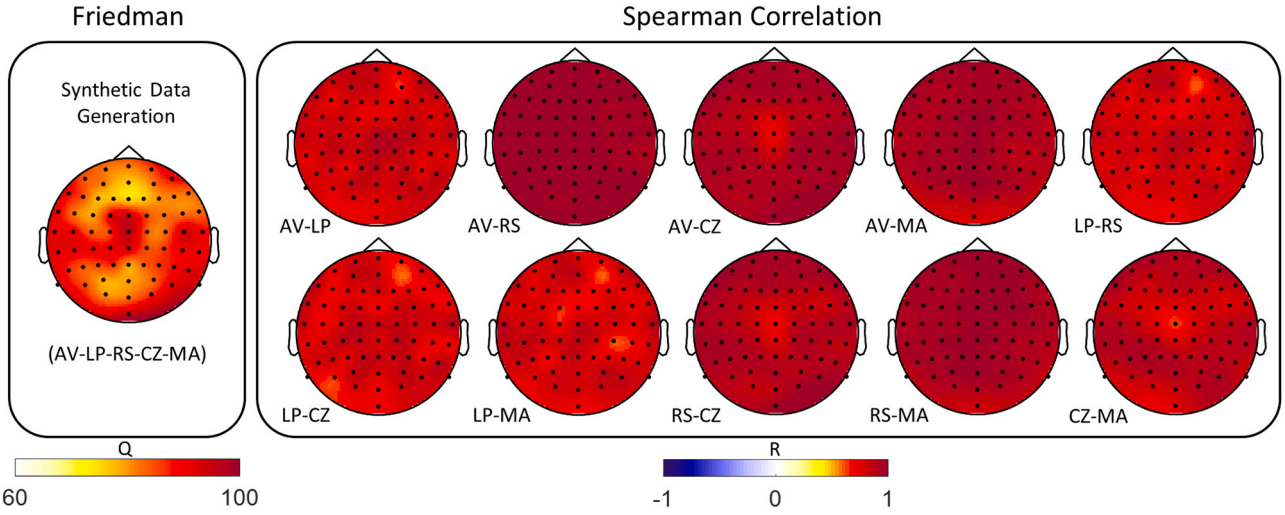

Fig. 3. Friedman test and Spearman Correlation analysis for the SDG method in the resting state dataset. The Friedman test was performed for all the EEG reference methods studied in this paper. The Friedman colormap corresponds to the Friedman stat (Q) obtained for individual channels. The Spearman Correlation colormaps correspond to the Correlation Coefficients (R) obtained among subjects per channel. In all topographies, electrodes resulting as statistically significant following a Bonferroni correction are shown as thick dots across the scalp.

Table 2
Group-wise Median(X) ± MAD(X) correlation coefficient among channels ($\overline{R}$) in all EEG reference pairs for the SDG method.

Pair	AV–LP	AV–RS	AV–CZ	AV–MA	LP–RS	LP–CZ	LP–MA	RS–CZ	RS–MA	CZ–MA
$\overline{R}$	0.81 ± 0.04	0.98 ± 0.01	0.93 ± 0.02	0.94 ± 0.02	0.81 ± 0.04	0.80 ± 0.06	0.79 ± 0.04	0.91 ± 0.03	0.96 ± 0.02	0.87 ± 0.04

Note: AV: Average, LP: Laplacian, RS: Reference Electrode Standardisation Technique, CZ: Vertex, MA: Mastoids Average.

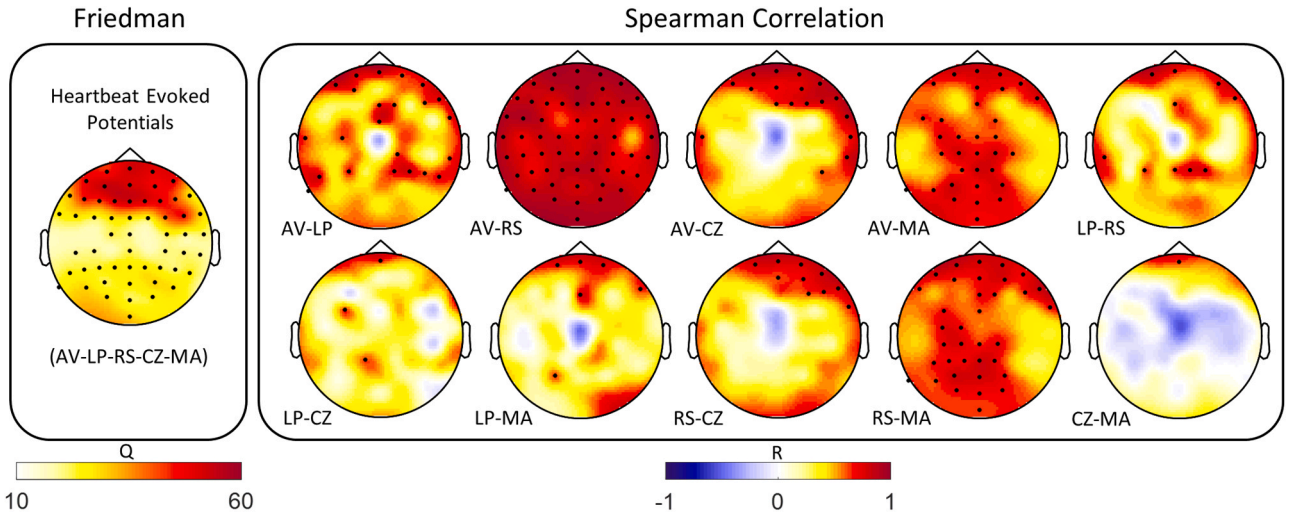

Fig. 4. Friedman test and Spearman Correlation analysis for the Heartbeat-evoked Potentials method in the resting-state dataset The Friedman test was performed for all the EEG reference methods studied in this paper. The Friedman colormap corresponds to the Friedman-stat (Q) obtained for individual channels. The Spearman Correlation colormaps correspond to the Correlation Coefficients (R) obtained among subjects per channel. In all topographies, electrodes resulting as statistically significant following a Bonferroni correction are shown as thick dots across the scalp.

Table 3
Median(X) ± MAD(X) correlation coefficient among channels ($\overline{R}$) in all EEG reference pairs for the Heartbeat-Evoked Potentials method.

Pair	AV–LP	AV–RS	AV–CZ	AV–MA	LP–RS	LP–CZ	LP–MA	RS–CZ	RS–MA	CZ–MA
$\overline{R}$	0.54 ± 0.12	0.84 ± 0.05	0.43 ± 0.18	0.62 ± 0.11	0.46 ± 0.13	0.33 ± 0.13	0.34 ± 0.14	0.39 ± 0.17	0.64 ± 0.09	0 ± 0.14

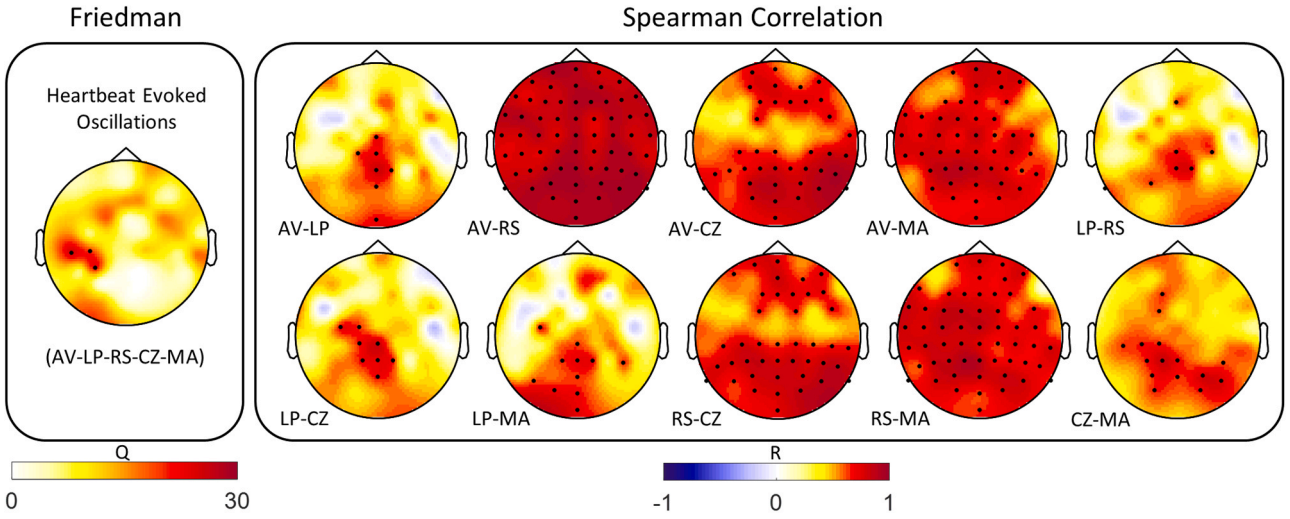

Fig. 5. Friedman test and Spearman correlation analysis for the heartbeat-evoked oscillations method in the resting-state dataset. The Friedman test was performed for all the EEG reference methods studied in this paper. The Friedman colormap corresponds to the Friedman-stat (Q) obtained for individual channels. The Spearman Correlation colormaps correspond to the Correlation Coefficients (R) obtained among subjects per channel. In all topographies, electrodes resulting as statistically significant following a Bonferroni correction are shown as thick dots across the scalp.

Table 4
Median(X) ± MAD(X)correlation coefficient among channels ($\overline{R}$) in all EEG reference pairs for the Heartbeat-Evoked Oscillations method.

Pair	AV–LP	AV–RS	AV–CZ	AV–MA	LP–RS	LP–CZ	LP–MA	RS–CZ	RS–MA	CZ–MA
$\overline{R}$	0.39 ± 0.16	0.87 ± 0.05	0.68 ± 0.12	0.72 ± 0.07	0.41 ± 0.16	0.41 ± 0.12	0.42 ± 0.16	0.68 ± 0.10	0.73 ± 0.07	0.53 ± 0.08

potentials, being LP and CZ the references causing major distortions.

3.1.4. Maximal information coefficient (MIC)

No significant changes occurred in the BHI index distribution, according to the results of the Friedman test in Fig. 6. Even then, the highest stats are in the frontal electrodes, as indicated by the SDG method and HEP. The median Spearman correlation coefficients range from 0.21 to 0.62, as shown in Table 5. MIC as computed with AV–RS presents the highest agreement, as in the other BHI methods, and LP–MA the lowest. As observed earlier, LP and CZ references affect this BHI method the most, as observed in Fig. 6, where the lowest correlations are found when MIC is computed with the LP and CZ references. To summarise Fig. 6, the results indicate that changing the EEG reference in the computation of MIC does not cause any major change in the index distributions, but it does generate massive distortions when measured in the correlation analysis, with the exception of the AV–RS reference.

3.2. Comparison between functional BHI assessment methodologies

To assess the overall similarity between BHI methods when computed through different EEG references, we performed for each EEG reference a Friedman test between the BHI methods and assessed the most divergent scalp regions in terms of the BHI index distribution among all subjects. The results are summarised in Fig. 7. Under resting state, the entire scalp appears significantly affected, with the frontal electrodes with the highest Friedman Q-stat for AV, CZ, MA, and RS. The LP reference has a consistent high effect size throughout the scalp, which means it is the EEG reference with least similarities among the BHI methods, as well as the most divergent EEG reference method given its varying topography. To confirm these findings, we performed the same analysis in the emotion elicitation dataset, for the emotions of joy and anger. Friedman's scalp topographies during joy elicitation presented a significant cluster in the midline parietal region, for AV, RS and CZ. Similarly, the same EEG references presented similarities for the anger elicitation trial in the three regions, with a relatively higher Friedman Q-stat—one left-frontal and another right-central and left-occipital. Nevertheless, none of them were statistically significant. Compared with other EEG references, the LP reference caused an inconsistent scalp topography in the three conditions studied, as observed in Fig. 7. This highlights the divergence of the LP reference with respect to other EEG reference methods for both the resting state and emotion elicitation.

3.3. Analysis of correlation between EEG references: resting state and emotion elicitation studies

We repeated the analysis of correlation between the EEG references over the emotion-elicitation dataset. This dataset considers the BHI's raw effect, which is the average BHI value during the emotion elicitation subtracted from the average BHI value during the rest period before the commencement of the video trial. With the two trials, joy and anger elicitations, we verified if the results head in the same direction as the resting state dataset. We selected the RS reference, as it agrees the most with the AV reference, and the LP reference, which agrees the least (for comparisons between other EEG references please see Supplementary Material).

Fig. 8 presents the scalp topographies for the AV–LP and AV–RS correlations for all BHI methods in the three datasets. Results of the SDG method showed overall high correlations as in resting state, but the anger-elicitation trial presented a reduced correlation between AV and LP. The results of HEP and HEO from emotion-elicitation data show the same trends. HEP computed with AV and LP references had a low correlation with each other, while computed with AV and RS references exhibited a high correlation. MIC also demonstrates the low correlations between AV and LP in the two trials of emotion elicitation. MIC computed with AV and RS references are more homogeneously correlated among the channels during emotion elicitation than during the resting state, where a few reduced correlations were observed towards both temporal regions. Nonetheless, MIC maintained the lowest correlations when changing the EEG reference, compared with the other BHI methods.

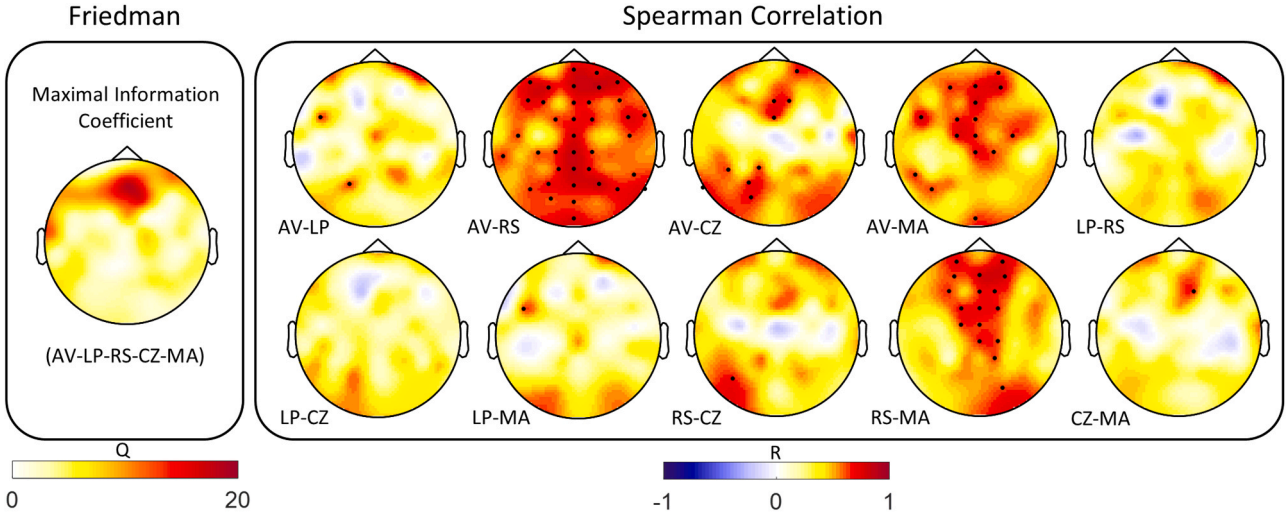

Fig. 6. Friedman test and Spearman correlation analysis for the maximal information coefficient method in the resting-state dataset. The Friedman test was performed for all the EEG reference methods studied in this paper. The Friedman colormap corresponds to the Friedman-stat (Q) obtained for individual channels. The Spearman Correlation colormaps correspond to the Correlation Coefficients (R) obtained among subjects per channel. In all topographies, electrodes resulting as statistically significant following a Bonferroni correction are shown as thick dots across the scalp.

Table 5
Median(X) ± MAD(X)correlation coefficient among channels ($\overline{R}$) in all EEG reference pairs for the Maximal Information Coefficient method.

Pair	AV–LP	AV–RS	AV–CZ	AV–MA	LP–RS	LP–CZ	LP–MA	RS–CZ	RS–MA	CZ–MA
$\overline{R}$	0.23 ± 0.13	0.62 ± 0.08	0.42 ± 0.15	0.51 ± 0.09	0.29 ± 0.10	0.25 ± 0.10	0.21 ± 0.12	0.36 ± 0.14	0.49 ± 0.11	0.24 ± 0.13

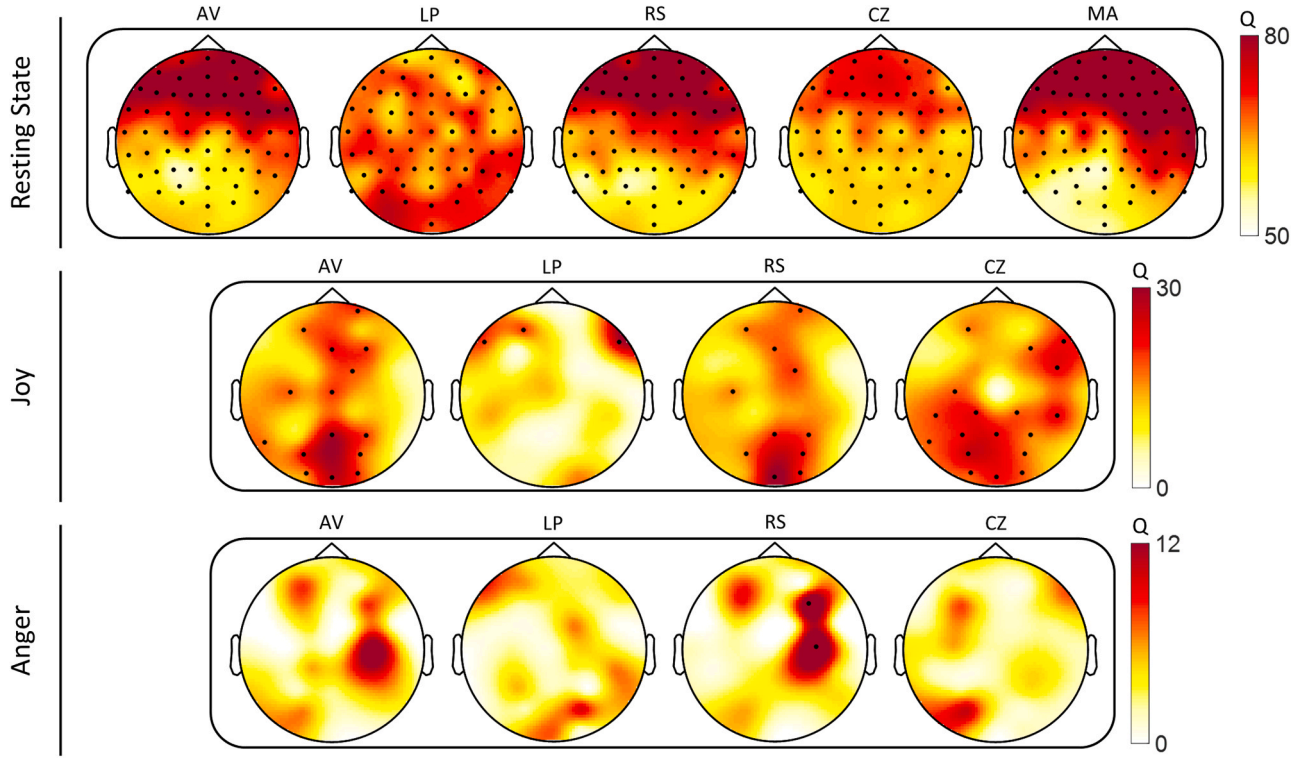

Fig. 7. Friedman test between BHI methods within each EEG reference, performed with three datasets—resting state, joy elicitation and anger elicitation. Colormaps indicate the Friedman-stat (Q). In all topographies, electrodes resulting as statistically significant following a Bonferroni correction are shown as thick dots across the scalp.

4. Discussion

A number of studies have stated that a suboptimal electrical re-reference of EEG data may cause distortions, including mis-measurements of event-related potentials, or bias the estimation of the EEG spectrogram (Hagemann et al., 2001; Kayser and Tenke, 2010; Hu et al., 2018). To help meet the important concerns about the electrical reference raised in existing EEG-related studies, this discussion aims to provide experts with use guidelines on the installation of an optimal EEG reference for the assessment of functional BHI. We analysed EEG power series in the alpha band (8–12 Hz) and HRV power series in the HF band gathered from healthy subjects during resting state and emotion elicitation. We are aware that emotional states may especially be characterised by BHI sustained by oscillations in different frequency bands, and a comprehensive investigation on the role of EEG references throughout EEG and HRV frequency bands in both functional directions, for different BHI estimation methodology, may be part of future endeavours (Candia-Rivera et al., 2021b).

Experimental results suggest that the SDG method provides consistent estimates with respect to different EEG references, while the MIC is the most sensitive quantifier. For the EEG references, while AV and RS should be preferred because of the consistency between the BHI estimation methods, the LP reference introduces major distortions in a functional BHI estimation.

4.1. Consistency between EEG references

The use of AV and RS re-references methods led to consistent results in terms of functional BHI estimation, compared with the other EEG references, as observed in Fig. 8, while MA, LP and CZ showed differences between different BHI methods.

The use of an AV reference is founded with a theoretical background, indicating that the integral of the surface potential of a volume conductor is zero (Offner, 1950). Experiments have revealed the independence of AV reference to specific locations on the scalp (Kayser and Tenke, 2010), as well as robustness to different experimental conditions (Bertrand et al., 1985). However, the AV reference is not always ideal, and may be affected by such factors as the number of EEG electrodes used for AV calculations (Bertrand et al., 1985).

The RS reference aims to standardize EEG to a point at infinity, based on a reference-independent approach of signal re-construction with respect to the equivalent sources from scalp EEG recordings (Yao, 2001). Though proven to be effective in capturing activity in the superficial cortical region, the RS reference faces challenges in high-noise conditions (Hu et al., 2018). Indeed, source reconstruction is not recommended in EEG with low signal-to-noise ratio (Cohen and Ridderinkhof, 2013; Michel and Brunet, 2019). The critical conditions required to ensure optimal AV reference estimation are a wide scalp coverage and a threshold for the number of channels.

The high agreement obtained between AV and RS reference could be owing to the experimental conditions of this study being sufficient to ensure an optimal reference, or more unlikely, these BHI markers

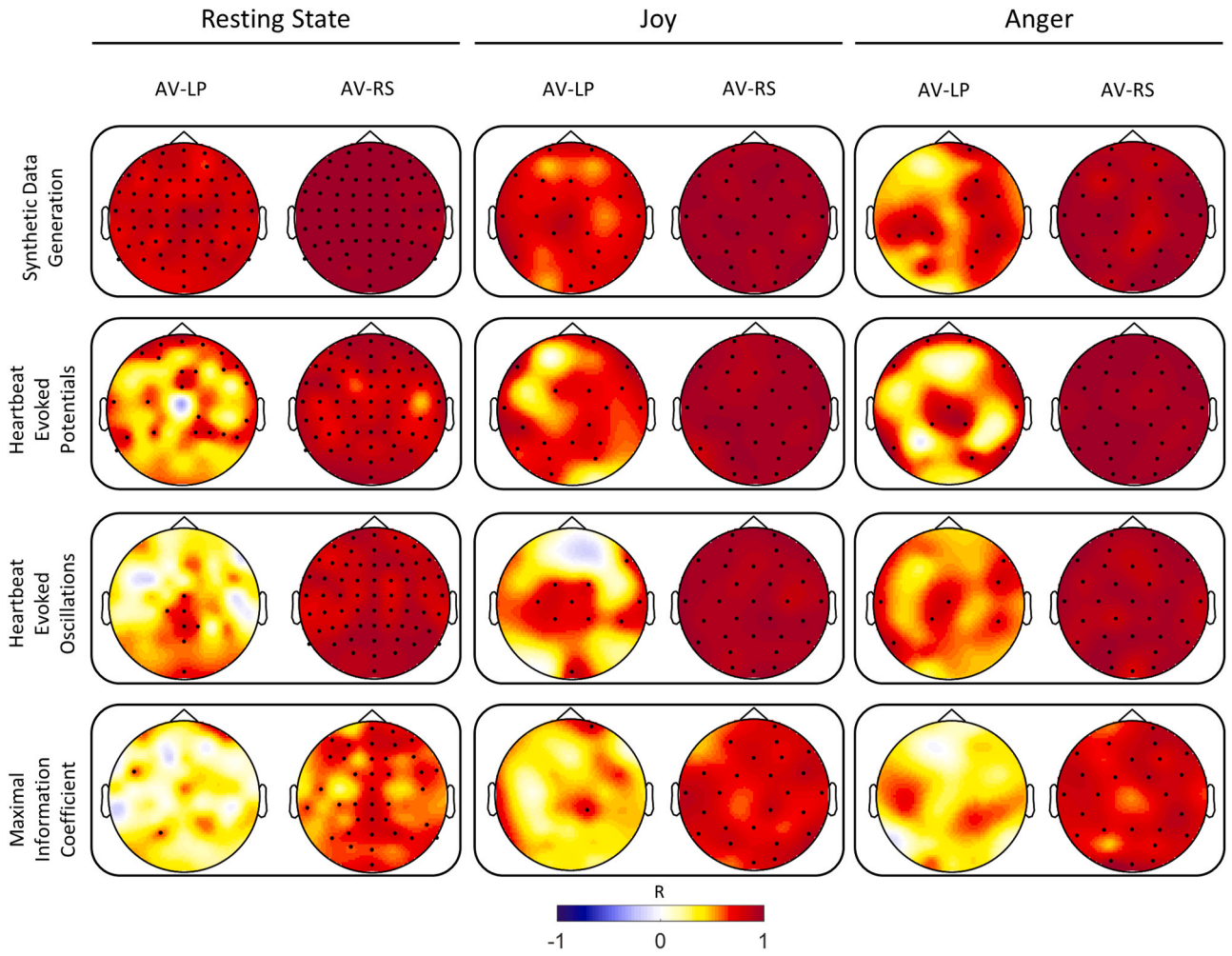

Fig. 8. Spearman correlation analysis for the BHI methods studied in resting state and emotion elicitation datasets for joy and anger. The correlations correspond to the result of the comparison of the AV reference with the LP and RS references. The Spearman Correlation colormaps correspond to the Correlation Coefficients (R) obtained among subjects per channel. In all topographies, electrodes resulting as statistically significant following a Bonferroni correction are shown as thick dots across the scalp.

studied are not affected by the aforementioned critical conditions.

The LP reference is computed through a linear combination of the data, estimating the changes in current density across the scalp, given the curvature of the brain's electrical field (Nunez, 1989). The LP reference proved to be the most divergent reference to compute all BHI markers studied (Fig. 7), which implies that the experimental and processing conditions did not meet the necessity of ensuring an optimal scalp current estimation through the LP method. The LP method is largely dependent on the number of EEG electrodes, as it is a preferred reference for use in high-density EEG (Nunez et al., 1994). Furthermore, the LP reference is computed through an analytical method which is significantly affected in high-noise conditions.

Finally, the use of single electrodes to reference EEG, such as the CZ, assumes that the specific single electrode taken as reference is a neutral point; however, CZ is electrically active and thus the use of single electrodes to reference EEG has been challenged (Lehmann, 1984; Hagemann et al., 2001). Indeed, Fig. 4 shows some electrodes with negative correlation coefficients when using samples associated with CZ reference. However, those estimates are not associated with a statistically significant correlation, and such negative fluctuations should then be considered as sampling fluctuations of the true correlation coefficients equal to 0. In this study, the use of CZ reference affected the measurement in nearby electrodes in the scalp's central region.

The case of the MA reference may be associated with a region of reduced neural activity with respect to other cephalic sites (Hagemann et al., 2001). However, previous studies revealed the inconsistent performances of MA references when compared with an AV reference (Hu et al., 2018). In this study, MA distorted the measurement of EEG activity in the temporal regions. Given that mastoids are located outside the scalp, the mastoid electrodes could capture brain activity in the temporal lobe (Stephenson and Gibbs, 1951), or even distort the measurement in nearby electrodes, given that the electromagnetic field generated on the mastoid electrodes may alter the flow of current in nearby regions (Miller et al., 1991).

4.2. *Region-specific effects*

To determine the scalp regions most affected by changing the EEG reference, for each EEG channel, we investigated group-wise differences between BHI assessment methods for a given EEG reference through a Friedman test. These results do not necessarily implicate a distortion in the BHI; rather, it shows changes in the range where values fluctuate with a possible constant relative displacement among the channels, maintaining a high correlation, as with the SDG method (Fig. 3).

SDG and HEP underwent the most changes in the marker distributions. Particularly, HEP showed more significant changes over frontal electrodes (Fig. 4, Friedman test). Previous studies have demonstrated the regions affected by changing of the EEG reference, which were

located at the frontal channels when measuring, for instance, the brain asymmetry (Hagemann et al., 2001). Regarding the most affected regions in the correlation analysis, HEP presented more disparities in the temporal electrodes in both hemispheres when using the MA reference and vertex region when using CZ reference (Fig. 4, Spearman correlation).

Interestingly, the results of the Friedman test revealed non-significant changes in the HEO and MIC distributions when changing the EEG reference (Figs. 5 and 6, respectively), while MIC was the most affected method in the correlation analysis. This is reasonable, knowing that these methods have a restricted range, as HEO measures a proportional change in the EEG power before the heartbeat, and MIC measures signal agreements, both have a range of 0–1. While the temporal regions and the whole scalp showed significant changes in the MIC correlation analysis when using an MA reference and LP or CZ references, respectively, frontal regions showed significant changes in the HEO correlation analysis when using a LP reference.

To determine the scalp regions most affected by changing the BHI estimation method computed with different EEG references, we performed the Friedman tests between the different BHI markers computed with the same EEG reference every time. Dataset I showed a more significant change between the BHI methods in the frontal regions, with the exception of cases with LP reference, where no focused effect was observed. Dataset II showed a significant cluster in the midline parietal channels for the joy-elicitation trial (Fig. 7). These results suggest the presence of latent functional BHI in the frontal channels during resting state. Indeed, the prefrontal and fronto-parietal cortex are known to be involved in the alpha band at rest (Sadaghiani et al., 2012; Stewart et al., 2014). Our results suggest that different BHI markers capture different ongoing physiological activities, and the coupling could be measured as brain–heart connectivity or coordination, directional modulations, or instantaneous responses.

On the emotion elicitation, our results show that BHI estimates in midline regions were significantly affected by a joy elicitation; further analyses are required to uncover the physiological meaning of these changes.

4.3. Sensitivity of functional BHI biomarkers

Estimates from the SDG method appears to have been affected only slightly (see Fig. 3, Spearman correlation). The robustness of SDG may be related to the way in which the indices are computed based on the relative changes of the two time series, rather than the specific amplitudes (Catrambone et al., 2019b).

Unlike SDG, the largest variety of distortions are found in HEP when changing the EEG reference, obtaining median correlation coefficients among channels in the range between 0 and 0.84 (Table 2). These results indicate that some EEG reference may severely change the measurement of HEP. As stated earlier, the EEG reference may affect considerably the amplitudes of scalp potentials (Lei and Liao, 2017). When measuring HEP, the correlation of the marker decreased when comparing any of the EEG references with either LP or CZ references (Fig. 4, Spearman correlation). The specific effects of these EEG references on scalp potentials have been described before; LP reference may be less accurate in expressing the different components of an event-related potential (Kayser and Tenke, 2015), whereas the CZ reference causes some disparities between these potentials as they are referenced to an active neural site (Lehmann, 1984; Hagemann et al., 2001).

Similarly, the effects on HEO when changing the EEG reference were mostly found when comparing one reference with LP or CZ. However, the median correlation coefficients in HEO are higher than in HEP. These results suggest that the distortions caused by the changing of the EEG reference are stronger in the scalp potentials than in the power spectrum amplitudes estimations. The previously reported event-related spectral changes caused by the EEG reference are related to the sum of linear and non-linear data transformations (Tenke and Kayser, 2005), even though the effects of LP reference on spectral data are related to reduced sharpness and a more even distribution across topographies (Kayser and Tenke, 2015).

On the other hand, MIC is the most affected method changing the EEG reference (Figs. 6 and 8). Similarly to SDG, it does not consider the specific amplitude. Therefore, we hypothesize two reasons explaining why the method is affected. First, the EEG reference may affect the subjects differently, because of different conditions such as noise level. This would be reflected in the correlation measures. However, the other BHI methods using spectral components of EEG did not go through these levels of distortions. Second, MIC may be affected because of how it is computed. MIC computation starts building an adapted grid in the time domain based on the curvatures presented in the time series compared (Fig. 2) (Reshef et al., 2011). Thereby, changes the EEG reference would result in changes in the time-frequency domain which would be translated in a different grid every time, leading to a different result.

5. Conclusions

The standardisation of methodologies in the assessment of functional BHI comes with the increasing use of these methods in important domains, such as clinical and methodological research and possible commercial applications. The results of this study suggest avoiding the use of the LP reference when performing a functional BHI assessment, supported by the high estimation variability caused by this EEG reference. In the same direction, the use of EEG references based on single, or a pair of channels may cause distortions related to localised noise, and the capture of neuronally active regions might generate an overall distortion.

We conclude that the AV and RS references are the safest options to be used in a quantitative, functional BHI study. However, an important issue to consider regarding the RS reference is the anatomical features, which in this study have been assumed to be constant, and the EEG sources. The sources are, however, part of future EEG studies with numerous constraints, especially with the possibility of high noise in the recordings. Noise is a sizeable concern, especially for studies performed in clinical environments, and the upcoming clinical applications of BHI may consider the same.

We conclude that the arbitrary use of EEG references may significantly distort the measurement of functional BHI, depending on the estimation method. We confirm the crucial role of EEG electrical reference and encourage researchers to consider using the AV reference with a wide scalp coverage for a functional BHI assessment.

Funding

The research leading to these results has received partial funding from the European Commission - Horizon 2020 Program under grant agreement n° 813234 of the project “RHUMBO”, and from the Italian Ministry of Education and Research (MIUR) in the framework of the CrossLab project (Departments of Excellence).

Ethical statement

The study was approved by the ethics committee at the University of Pisa. All subjects signed an informed consent for approval of participation in the study, as required by the declaration of Helsinki.

CRediT authorship contribution statement

Authors declare no competing interests. Individual authors’ contributions are: **G.V.** conceived the study. **V.C.** recorded the data. **D.C.-R.** processed the data. **D.C.-R.**, **V.C.** and **G.V.** analysed the data. **D.C.-R.**, **V.C.** and **G.V.** wrote the paper.

Declaration of Competing Interest

Authors declare no competing interests.

Appendix A. Supporting information

Supplementary data associated with this article can be found in the online version at doi:10.1016/j.jneumeth.2021.109269.

References

Acharya, U.R., Paul Joseph, K., Kannathal, N., Lim, C.M., Suri, J.S., 2006. Heart rate variability: a review. Med. Biol. Eng. Comput. 44, 1031–1051.

Al, E., Iliopoulos, F., Forschack, N., Nierhaus, T., Grund, M., Motyka, P., Gaebler, M., Nikulin, V.V., Villringer, A., 2020. Heart–brain interactions shape somatosensory perception and evoked potentials. PNAS 117, 10575–10584.

Al-Nashash, H., Al-Assaf, Y., Paul, J., Thakor, N., 2004. EEG signal modeling using adaptive Markov process amplitude. IEEE Trans. Biomed. Eng. 51, 744–751.

Azzalini, D., Buot, A., Palminteri, S., Tallon-Baudry, C., 2021. Responses to heartbeats in ventromedial prefrontal cortex contribute to subjective preference-based decisions. J. Neurosci. 41, 5102–5114.

Azzalini, D., Rebollo, I., Tallon-Baudry, C., 2019. Visceral signals shape brain dynamics and cognition. Trends Cogn. Sci. 23, 488–509.

Babo-Rebelo, M., Richter, C.G., Tallon-Baudry, C., 2016. Neural responses to heartbeats in the default network encode the self in spontaneous thoughts. J. Neurosci. 36, 7829–7840.

Balconi, M., Falbo, L., Brambilla, E., 2009. BIS/BAS responses to emotional cues: self report, autonomic measure and alpha band modulation. Personal. Individ. Differ. 47, 858–863.

Bashan, A., Bartsch, R.P., Kantelhardt, J.W., Havlin, S., Ivanov, P.C., 2012. Network physiology reveals relations between network topology and physiological function. Nat. Commun. 3, 702.

Beissner, F., Meissner, K., Bär, K.-J., Napadow, V., 2013. The autonomic brain: an activation likelihood estimation meta-analysis for central processing of autonomic function. J. Neurosci. 33, 10503–10511.

Bertrand, O., Perrin, F., Pernier, J., 1985. A theoretical justification of the average reference in topographic evoked potential studies. Electroencephalogr. Clin. Neurophysiol./Evoked Potentials Sect. 62, 462–464.

Blanke, O., Slater, M., Serino, A., 2015. Behavioral, neural, and computational principles of bodily self-consciousness. Neuron 88, 145–166.

Brennan, M., Palaniswami, M., Kamen, P., 2002. Poincaré plot interpretation using a physiological model of HRV based on a network of oscillators. Am. J. Physiol. Heart Circ. Physiol. 283, H1873–H1886.

Calandra-Buonaura, G., Toschi, N., Provini, F., Corazza, I., Bisulli, F., Barletta, G., Vandi, S., Montagna, P., Guerrisi, M., Tinuper, P., Cortelli, P., 2012. Physiologic autonomic arousal heralds motor manifestations of seizures in nocturnal frontal lobe epilepsy: implications for pathophysiology. Sleep Med. 13, 252–262.

Candia-Rivera, D., Annen, J., Gosseries, O., Martial, C., Thibaut, A., Laureys, S., Tallon-Baudry, C., 2021a. Neural responses to heartbeats detect residual signs of consciousness during resting state in post-comatose patients. J. Neurosci. 41, 5251–5262.

Candia-Rivera, D., Catrambone, V., Thayer, J.F., Gentili, C., Valenza, G., 2021b. Cardiac sympathovagal activity initiates a functional brain-body response to emotional processing. bioRxiv, 2021.06.05.447188.

Candia-Rivera D., Catrambone V., Valenza G. , 2020a. The role of EEG electrical reference in the assessment of functional brain-heart interplay: a preliminary study. In: 2020 11th Conference of the European Study Group on Cardiovascular Oscillations (ESGCO), pp. 1–2.

Candia-Rivera D., Catrambone V., Valenza G. , 2020b. Methodological considerations on EEG electrical reference: a functional brain-heart interplay study. In: 2020 42nd Annual International Conference of the IEEE Engineering in Medicine Biology Society (EMBC), pp. 553–556.

Carvalhaes, C., de Barros, J.A., 2015. The surface Laplacian technique in EEG: theory and methods. Int. J. Psychophysiol. 97, 174–188.

Catrambone, V., Greco, A., Scilingo, E.P., Valenza, G., 2019a. Functional linear and nonlinear brain–heart interplay during emotional video elicitation: a maximum information coefficient study. Entropy 21, 892.

Catrambone, V., Greco, A., Vanello, N., Scilingo, E.P., Valenza, G., 2019b. Time-resolved directional brain-heart interplay measurement through synthetic data generation models. Ann. Biomed. Eng. 47, 1479–1489.

Catrambone, V., Messerotti Benvenuti, S., Gentili, C., Valenza, G., 2021a. Intensification of functional neural control on heartbeat dynamics in subclinical depression. Transl. Psychiatry 11, 1–10.

Catrambone, V., Talebi, A., Barbieri, R., Valenza, G., 2021b. Time-resolved brain-to-heart probabilistic information transfer estimation using inhomogeneous point-process models. IEEE Trans. Biomed. Eng. 1. In press/Early access.

Catrambone V., Wendt H., Barbieri R., Abry P., Valenza G. , 2020. Quantifying functional links between brain and heartbeat dynamics in the multifractal domain: a preliminary analysis. In: 2020 42nd Annual International Conference of the IEEE Engineering in Medicine Biology Society (EMBC), pp. 561–564.

Chen, W.G., Schloesser, D., Arensdorf, A.M., Simmons, J.M., Cui, C., Valentino, R., Gnadt, J.W., Nielsen, L., Hillaire-Clarke, C.St, Spruance, V., Horowitz, T.S., Vallejo, Y.F., Langevin, H.M., 2021. The emerging science of interoception: sensing, integrating, interpreting, and regulating signals within the self. Trends Neurosci. 44, 3–16.

Cohen, M.X., Ridderinkhof, K.R., 2013. EEG source reconstruction reveals frontal-parietal dynamics of spatial conflict processing. PLoS One 8, e57293.

Costa, A.H., Boudreau-Bartels, G.F., 1995. Design of time-frequency representations using a multiform, tiltable exponential kernel. IEEE Trans. Signal Process. 43, 2283–2301.

Craig, A.D., 2002. How do you feel? Interoception: the sense of the physiological condition of the body. Nat. Rev. Neurosci. 3, 655–666.

Craig, A.D., 2009. How do you feel — now? The anterior insula and human awareness. Nat. Rev. Neurosci. 10, 59–70.

Craig, A.D.B., 2003. Pain mechanisms: labeled lines versus convergence in central processing. Annu. Rev. Neurosci. 26, 1–30.

Critchley, H.D., Harrison, N.A., 2013. Visceral influences on brain and behavior. Neuron 77, 624–638.

Damasio, A., 1999. The Feeling of What Happens: Body and Emotion in the Making of Consciousness. Harcourt College Publishers, Fort Worth, TX, US.

Damasio, A., 2010. Self Comes to Mind: Constructing the Conscious Brain. Pantheon/Random House, New York, NY, US.

de Munck, J.C., Gonçalves, S.I., Faes, Th.J.C., Kuijer, J.P.A., Pouwels, P.J.W., Heethaar, R.M., Lopes da Silva, F.H., 2008. A study of the brain's resting state based on alpha band power, heart rate and fMRI. NeuroImage 42, 112–121.

Desmedt, J.E., Chalklin, V., Tomberg, C., 1990. Emulation of somatosensory evoked potential (SEP) components with the 3-shell head model and the problem of 'ghost potential fields' when using an average reference in brain mapping. Electroencephalogr. Clin. Neurophysiol./Evoked Potentials Sect. 77, 243–258.

Dien, J., 1998. Issues in the application of the average reference: review, critiques, and recommendations. Behav. Res. Methods Instrum. Comput. 30, 34–43.

Dirlich, G., Vogl, L., Plaschke, M., Strian, F., 1997. Cardiac field effects on the EEG. Electroencephalogr. Clin. Neurophysiol. 102, 307–315.

Dumont, M., Jurysta, F., Lanquart, J.-P., Migeotte, P.-F., van de Borne, P., Linkowski, P., 2004. Interdependency between heart rate variability and sleep EEG: linear/non-linear? Clin. Neurophysiol. 115, 2031–2040.

Esler, M.D., 1998. Mental stress, panic disorder and the heart. Stress Med. 14, 237–243.

Faes, L., Marinazzo, D., Jurysta, F., Nollo, G., 2015. Linear and non-linear brain-heart and brain-brain interactions during sleep. Physiol. Meas. 36, 683–698.

Faes, L., Nollo, G., Jurysta, F., Marinazzo, D., 2014. Information dynamics of brain–heart physiological networks during sleep. New J. Phys. 16, 105005.

Fein, G., Raz, J., Brown, F.F., Merrin, E.L., 1988. Common reference coherence data are confounded by power and phase effects. Electroencephalogr. Clin. Neurophysiol. 69, 581–584.

Gabard-Durnam, L.J., Mendez Leal, A.S., Wilkinson, C.L., Levin, A.R., 2018. The Harvard Automated Processing Pipeline for Electroencephalography (HAPPE): standardized processing software for developmental and high-artifact data. Front. Neurosci. 12. Available at: https://www.frontiersin.org/articles/10.3389/fnins.2018.00097/full.

Greco, A., Faes, L., Catrambone, V., Barbieri, R., Scilingo, E.P., Valenza, G., 2019. Lateralization of directional brain-heart information transfer during visual emotional elicitation. Am. J. Physiol.-Regul. Integr. Comp. Physiol. 317, R25–R38.

Grosselin, F., Navarro-Sune, X., Raux, M., Similowski, T., Chavez, M., 2018. CARE-rCortex: a Matlab toolbox for the analysis of CArdio-REspiratory-related activity in the cortex. J. Neurosci. Methods 308, 309–316.

Hagemann, D., Naumann, E., Becker, G., Maier, S., Bartussek, D., 1998. Frontal brain asymmetry and affective style: a conceptual replication. Psychophysiology 35, 372–388.

Hagemann, D., Naumann, E., Thayer, J.F., 2001. The quest for the EEG reference revisited: a glance from brain asymmetry research. Psychophysiology 38, 847–857.

He, B., Lian, J., Li, G., 2001. High-resolution EEG: a new realistic geometry spline Laplacian estimation technique. Clin. Neurophysiol. 112, 845–852.

Hu S., Cao Y., Chen S., Kong W., Zhang J., Li X., Zhang Y. , 2012. Independence verification for reference signal under neck of human body in EEG recordings. In: Proceedings of the 31st Chinese Control Conference, pp. 4038–4043.

Hu, S., Lai, Y., Valdes-Sosa, P.A., Bringas-Vega, M.L., Yao, D., 2018. How do reference montage and electrodes setup affect the measured scalp EEG potentials? J. Neural Eng. 15, 026013.

Hu, S., Stead, M., Dai, Q., Worrell, G.A., 2010. On the recording reference contribution to EEG correlation, phase synchorony, and coherence. IEEE Trans. Syst. Man Cybern. Part B (Cybern.) 40, 1294–1304.

Huiskamp, G., 1991. Difference formulas for the surface Laplacian on a triangulated surface. J. Comput. Phys. 95, 477–496.

Jiang, X., Zhang, Z., Ye, C., Lei, Y., Wu, L., Zhang, Y., Chen, Y., Xiao, Z., 2015. Attenuated or absent HRV response to postural change in subjects with primary insomnia. Physiol. Behav. 140, 127–131.

Junghöfer, M., Elbert, T., Tucker, D.M., Braun, C., 1999. The polar average reference effect: a bias in estimating the head surface integral in EEG recording. Clin. Neurophysiol. 110, 1149–1155.

Karavidas, M.K., Lehrer, P.M., Vaschillo, E., Vaschillo, B., Marin, H., Buyske, S., Malinovsky, I., Radvanski, D., Hassett, A., 2007. Preliminary results of an open label study of heart rate variability biofeedback for the treatment of major depression. Appl. Psychophysiol. Biofeedback 32, 19–30.

Kayser, J., Tenke, C.E., 2010. In search of the Rosetta Stone for scalp EEG: converging on reference-free techniques. Clin. Neurophysiol. 121, 1973–1975.

Kayser, J., Tenke, C.E., 2015. Issues and considerations for using the scalp surface Laplacian in EEG/ERP research: a tutorial review. Int. J. Psychophysiol. 97, 189–209.

Kayser, J., Tenke, C.E., Gates, N.A., Bruder, G.E., 2007. Reference-independent ERP old/new effects of auditory and visual word recognition memory: joint extraction of

stimulus- and response-locked neuronal generator patterns. Psychophysiology 44, 949–967.
Kim, J., Jeong, B., 2019. Heartbeat induces a cortical theta-synchronized network in the resting state. eNeuro 6. ENEURO.0200-19.2019.
Kim, J., Park, H.-D., Kim, K.W., Shin, D.W., Lim, S., Kwon, H., Kim, M.-Y., Kim, K., Jeong, B., 2019. Sad faces increase the heartbeat-associated interoceptive information flow within the salience network: a MEG study. Sci. Rep. 9, 430.
Lechinger, J., Heib, D.P.J., Gruber, W., Schabus, M., Klimesch, W., 2015. Heartbeat-related EEG amplitude and phase modulations from wakefulness to deep sleep: interactions with sleep spindles and slow oscillations. Psychophysiology 52, 1441–1450.
Lehmann, D., 1984. EEG assessment of brain activity: spatial aspects, segmentation and imaging. Int. J. Psychophysiol. 1, 267–276.
Lei, X., Liao, K., 2017. Understanding the influences of EEG reference: a large-scale brain network perspective. Front Neurosci. 11. Available at: ⟨https://www.frontiersin.org/articles/10.3389/fnins.2017.00205/full⟩.
Leistedt, S.J.-J., Linkowski, P., Lanquart, J.-P., Mietus, J.E., Davis, R.B., Goldberger, A.L., Costa, M.D., 2011. Decreased neuroautonomic complexity in men during an acute major depressive episode: analysis of heart rate dynamics. Transl. Psychiatry 1, e27.
Luu P., Ferree TC , 2000. Determination of the Geodesic Sensor Nets' Average Electrode Positions and Their 10 – 10 International Equivalents. Available at: ⟨https://www.egi.com/images/HydroCelGSN_10–10.pdf⟩ [Accessed April 6, 2018].
Magosso, E., Ricci, G., Ursino, M., 2019. Modulation of brain alpha rhythm and heart rate variability by attention-related mechanisms. AIMS Neurosci. 6, 1–24.
Martin, J.L.R., Martín-Sánchez, E., 2012. Systematic review and meta-analysis of vagus nerve stimulation in the treatment of depression: variable results based on study designs. Eur. Psychiatry 27, 147–155.
Marzetti, L., Nolte, G., Perrucci, M.G., Romani, G.L., Del Gratta, C., 2007. The use of standardized infinity reference in EEG coherency studies. Neuroimage 36, 48–63.
Michel, C.M., Brunet, D., 2019. EEG source imaging: a practical review of the analysis steps. Front. Neurol. 10. Available at: ⟨https://www.frontiersin.org/articles/10.3389/fneur.2019.00325/full⟩.
Miller, G.A., Lutzenberger, W., Elbert, T., 1991. The linked-reference issue in EEG and ERP recording. J. Psychophysiol. 5, 273–276.
Montoya, P., Schandry, R., Müller, A., 1993. Heartbeat evoked potentials (HEP): topography and influence of cardiac awareness and focus of attention. Electroencephalogr. Clin. Neurophysiol./Evoked Potentials Sect. 88, 163–172.
Nunez, P.L., 1989. Estimation of large scale neocortical source activity with EEG surface Laplacians. Brain Topogr. 2, 141–154.
Nunez, P.L., Silberstein, R.B., Cadusch, P.J., Wijesinghe, R.S., Westdorp, A.F., Srinivasan, R., 1994. A theoretical and experimental study of high resolution EEG based on surface Laplacians and cortical imaging. Electroencephalogr. Clin. Neurophysiol. 90, 40–57.
Offner, F.F., 1950. The EEG as potential mapping: the value of the average monopolar reference. Electroencephalogr. Clin. Neurophysiol. 2, 213–214.
Oostendorp, T.F., van Oosterom, A., 1996. The surface Laplacian of the potential: theory and application. IEEE Trans. Biomed. Eng. 43, 394–405.
Oostenveld, R., Fries, P., Maris, E., Schoffelen, J.-M., 2011. FieldTrip: open source software for advanced analysis of MEG, EEG, and invasive electrophysiological data. Comput. Intell. Neurosci. 2011, 1–9.
Orini, M., Bailón, R., Mainardi, L.T., Laguna, P., Flandrin, P., 2012. Characterization of dynamic interactions between cardiovascular signals by time-frequency coherence. IEEE Trans. Biomed. Eng. 59, 663–673.
Pace-Schott, E.F., Amole, M.C., Aue, T., Balconi, M., Bylsma, L.M., Critchley, H., Demaree, H.A., Friedman, B.H., Gooding, A., Gosseries, O., Jovanovic, T., Kirby, L., Kozlowska, K., Laureys, S., Lowe, L., Magee, K., Marin, M.F., Merner, A.R., Robinson, J.L., Smith, R.C., Spangler, D.P., Van Overveld, M., VanElzakker, M.B., 2019. Physiological feelings. Neurosci. Biobehav. Rev. 103, 267–304.
Park, H.-D., Bernasconi, F., Bello-Ruiz, J., Pfeiffer, C., Salomon, R., Blanke, O., 2016. Transient modulations of neural responses to heartbeats covary with bodily self-consciousness. J. Neurosci. 36, 8453–8460.
Park, H.-D., Bernasconi, F., Salomon, R., Tallon-Baudry, C., Spinelli, L., Seeck, M., Schaller, K., Blanke, O., 2018. Neural sources and underlying mechanisms of neural responses to heartbeats, and their role in bodily self-consciousness: an intracranial EEG study. Cereb. Cortex 28, 2351–2364.
Park, H.-D., Blanke, O., 2019. Heartbeat-evoked cortical responses: Underlying mechanisms, functional roles, and methodological considerations. NeuroImage 197, 502–511.
Park, H.-D., Correia, S., Ducorps, A., Tallon-Baudry, C., 2014. Spontaneous fluctuations in neural responses to heartbeats predict visual detection. Nat. Neurosci. 17, 612–618.
Park, H.-D., Tallon-Baudry, C., 2014. The neural subjective frame: from bodily signals to perceptual consciousness. Philos. Trans. R. Soc. Lond. Ser. B Biol. Sci. 369, 20130208.
Pascual-Marqui, R.D., Lehmann, D., 1993. Topographic maps, source localization inference, and the reference electrode: comments on a paper by Desmedt et al. Electro Clin. Neurophysiol. 88, 532–536.
Penninx, B.W., Milaneschi, Y., Lamers, F., Vogelzangs, N., 2013. Understanding the somatic consequences of depression: biological mechanisms and the role of depression symptom profile. BMC Med. 11, 129.
Perogamvros, L., Park, H.-D., Bayer, L., Perrault, A.A., Blanke, O., Schwartz, S., 2019. Increased heartbeat-evoked potential during REM sleep in nightmare disorder. NeuroImage: Clin. 22, 101701.
Picton, T.W., Bentin, S., Berg, P., Donchin, E., Hillyard, S.A., Johnson, R., Miller, G.A., Ritter, W., Ruchkin, D.S., Rugg, M.D., Taylor, M.J., 2000. Guidelines for using human event-related potentials to study cognition: Recording standards and publication criteria. Psychophysiology 37, 127–152.
Pollatos, O., Kirsch, W., Schandry, R., 2005. Brain structures involved in interoceptive awareness and cardioafferent signal processing: A dipole source localization study. Hum. Brain Mapp. 26, 54–64.
Porges, S.W., Doussard-Roosevelt, J.A., Maiti, A.K., 1994. Vagal tone and the physiological regulation of emotion. Monogr. Soc. Res. Child Dev. 59, 167–186.
Pyner, S., 2014. The paraventricular nucleus and heart failure. Exp. Physiol. 99, 332–339.
Qin, Y., Xu, P., Yao, D., 2010. A comparative study of different references for EEG default mode network: the use of the infinity reference. Clin. Neurophysiol. 121, 1981–1991.
Quigley, K.S., Kanoski, S., Grill, W.M., Barrett, L.F., Tsakiris, M., 2021. Functions of interoception: from energy regulation to experience of the self. Trends Neurosci. 44, 29–38.
Raimondo, F., Rohaut, B., Demertzi, A., Valente, M., Engemann, D.A., Salti, M., Slezak, D.F., Naccache, L., Sitt, J.D., 2017. Brain–heart interactions reveal consciousness in noncommunicating patients. Ann. Neurol. 82, 578–591.
Ray, W.J., Cole, H.W., 1985. EEG alpha activity reflects attentional demands, and beta activity reflects emotional and cognitive processes. Science 228, 750–752.
Reshef, D.N., Reshef, Y.A., Finucane, H.K., Grossman, S.R., McVean, G., Turnbaugh, P.J., Lander, E.S., Mitzenmacher, M., Sabeti, P.C., 2011. Detecting novel associations in large datasets. Science 334, 1518–1524.
Russell, J.A., 1980. A circumplex model of affect. J. Personal. Soc. Psychol. 39, 1161–1178.
Sadaghiani, S., Scheeringa, R., Lehongre, K., Morillon, B., Giraud, A.-L., D'Esposito, M., Kleinschmidt, A., 2012. Alpha-band phase synchrony is related to activity in the fronto-parietal adaptive control network. J. Neurosci. 32, 14305–14310.
Salamone, P.C., Legaz, A., Sedeño, L., Moguilner, S., Fraile-Vazquez, M., Campo, C.G., Fittipaldi, S., Yoris, A., Miranda, M., Birba, A., Galiani, A., Abrevaya, S., Neely, A., Caro, M.M., Alifano, F., Villagra, R., Anunziata, F., Okada de Oliveira, M., Pautassi, R.M., Slachevsky, A., Serrano, C., García, A.M., Ibañez, A., 2021. Interoception primes emotional processing: multimodal evidence from neurodegeneration. J. Neurosci. 41, 4276–4292.
Salamone, P.C., Sedeño, L., Legaz, A., Bekinschtein, T., Martorell, M., Adolfi, F., Fraile-Vazquez, M., Rodríguez Arriagada, N., Favaloro, L., Peradejordi, M., Absi, D.O., García, A.M., Favaloro, R., Ibáñez, A., 2020. Dynamic neurocognitive changes in interoception after heart transplant. Brain Commun. 2. https://doi.org/10.1093/braincomms/fcaa095.
Salvioli, B., Pellegatta, G., Malacarne, M., Pace, F., Malesci, A., Pagani, M., Lucini, D., 2015. Autonomic nervous system dysregulation in irritable bowel syndrome. Neurogastroenterol. Motil. 27, 423–430.
Samuels, M.A., 2007. The brain–heart connection. Circulation 116, 77–84.
Sanchez-Gonzalez, M.A., Guzik, P., May, R.W., Koutnik, A.P., Hughes, R., Muniz, S., Kabbaj, M., Fincham, F.D., 2015. Trait anxiety mimics age-related cardiovascular autonomic modulation in young adults. J. Hum. Hypertens. 29, 274–280.
Schandry, R., Montoya, P., 1996. Event-related brain potentials and the processing of cardiac activity. Biol. Psychol. 42, 75–85.
Schandry, R., Sparrer, B., Weitkunat, R., 1986. From the heart to the brain: a study of heartbeat contingent scalp potentials. Int J. Neurosci. 30, 261–275.
Schiecke, K., Schumann, A., Benninger, F., Feucht, M., Baer, K.-J., Schlattmann, P., 2019. Brain-heart interactions considering complex physiological data: processing schemes for time-variant, frequency-dependent, topographical and statistical examination of directed interactions by convergent cross mapping. Physiol. Meas. 40, 114001.
Schulz, S., Haueisen, J., Bär, K.-J., Voss, A., 2019. Altered causal coupling pathways within the central-autonomic-network in patients suffering from schizophrenia. Entropy 21, 733.
Sel, A., Azevedo, R.T., Tsakiris, M., 2017. Heartfelt self: cardio-visual integration affects self-face recognition and interoceptive cortical processing. Cereb. Cortex 27, 5144–5155.
Silvani, A., Calandra-Buonaura, G., Dampney, R.A.L., Cortelli, P., 2016. Brain-heart interactions: physiology and clinical implications. Philos. Trans. R. Soc. A: Math. Phys. Eng. Sci. 374, 20150181.
Soleymani, M., Lichtenauer, J., Pun, T., Pantic, M., 2012. A multimodal database for affect recognition and implicit tagging. IEEE Trans. Affect. Comput. 3, 42–55.
Srinivasan, R., Nunez, P.L., Silberstein, R.B., 1998. Spatial filtering and neocortical dynamics: estimates of EEG coherence. IEEE Trans. Biomed. Eng. 45, 814–826.
Stephenson, W.A., Gibbs, F.A., 1951. A balanced non-cephalic reference electrode. Electro Clin. Neurophysiol. 3, 237–240.
Stewart, J.L., Coan, J.A., Towers, D.N., Allen, J.J.B., 2014. Resting and task-elicited prefrontal EEG alpha asymmetry in depression: support for the capability model. Psychophysiology 51, 446–455.
Taggart, P., Boyett, M.R., Logantha, S.J.R.J., Lambiase, P.D., 2011. Anger, emotion, and arrhythmias: from brain to heart. Front Physiol. 2. Available at: ⟨https://www.ncbi.nlm.nih.gov/pmc/articles/PMC3196868/⟩.
Tahsili-Fahadan, P., Geocadin, R.G., 2017. Heart-brain axis: effects of neurologic injury on cardiovascular function. Circ. Res 120, 559–572.
Tallon-Baudry, C., Campana, F., Park, H.-D., Babo-Rebelo, M., 2018. The neural monitoring of visceral inputs, rather than attention, accounts for first-person perspective in conscious vision. Cortex 102, 139–149.
Tenke, C.E., Kayser, J., 2005. Reference-free quantification of EEG spectra: combining current source density (CSD) and frequency principal components analysis (fPCA). Clin. Neurophysiol. 116, 2826–2846.
Terhaar, J., Viola, F.C., Bär, K.-J., Debener, S., 2012. Heartbeat evoked potentials mirror altered body perception in depressed patients. Clin. Neurophysiol. 123, 1950–1957.

Thayer, J.F., Ahs, F., Fredrikson, M., Sollers, J.J., Wager, T.D., 2012. A meta-analysis of heart rate variability and neuroimaging studies: implications for heart rate variability as a marker of stress and health. Neurosci. Biobehav Rev. 36, 747–756.
Thayer, J.F., Lane, R.D., 2009. Claude Bernard and the heart–brain connection: further elaboration of a model of neurovisceral integration. Neurosci. Biobehav. Rev. 33, 81–88.
Valenza, G., Citi, L., Garcia, R.G., Taylor, J.N., Toschi, N., Barbieri, R., 2017. Complexity variability assessment of nonlinear time-varying cardiovascular control. Sci. Rep. 7, 42779.
Valenza, G., Citi, L., Gentili, C., Lanatá, A., Scilingo, E.P., Barbieri, R., 2014a. Point-process nonlinear autonomic assessment of depressive states in bipolar patients. Methods Inf. Med. 53, 296–302.
Valenza, G., Citi, L., Lanatá, A., Scilingo, E.P., Barbieri, R., 2014b. Revealing real-time emotional responses: a personalized assessment based on heartbeat dynamics. Sci. Rep. 4, 4998.
Valenza, G., Garcia, R.G., Citi, L., Scilingo, E.P., Tomaz, C.A., Barbieri, R., 2015. Nonlinear digital signal processing in mental health: characterization of major depression using instantaneous entropy measures of heartbeat dynamics. Front. Physiol. 6, 74.
Valenza, G., Greco, A., Gentili, C., Lanata, A., Sebastiani, L., Menicucci, D., Gemignani, A., Scilingo, E.P., 2016a. Combining electroencephalographic activity and instantaneous heart rate for assessing brain–heart dynamics during visual emotional elicitation in healthy subjects. Philos. Trans. R. Soc. A: Math. Phys. Eng. Sci. 374, 20150176.
Valenza, G., Nardelli, M., Lanata', A., Gentili, C., Bertschy, G., Kosel, M., Scilingo, E.P., 2016b. Predicting mood changes in bipolar disorder through heartbeat nonlinear dynamics. IEEE J. Biomed. Health Inf. 20, 1034–1043.
Valenza, G., Orsolini, S., Diciotti, S., Citi, L., Scilingo, E.P., Guerrisi, M., Danti, S., Lucetti, C., Tessa, C., Barbieri, R., Toschi, N., 2016c. Assessment of spontaneous cardiovascular oscillations in Parkinson's disease. Biomed. Signal Process. Control 26, 80–89.
Valenza, G., Passamonti, L., Duggento, A., Toschi, N., Barbieri, R., 2020. Uncovering complex central autonomic networks at rest: a functional magnetic resonance imaging study on complex cardiovascular oscillations. J. R. Soc. Interface 17, 20190878.
Valenza, G., Sclocco, R., Duggento, A., Passamonti, L., Napadow, V., Barbieri, R., Toschi, N., 2019. The central autonomic network at rest: uncovering functional MRI correlates of time-varying autonomic outflow. NeuroImage 197, 383–390.
Vehkaoja, A., Rajala, S., Kumpulainen, P., Lekkala, J., 2013. Correlation approach for the detection of the heartbeat intervals using force sensors placed under the bed posts. J. Med. Eng. Technol. 37, 327–333.
Wolpaw, J.R., Wood, C.C., 1982. Scalp distribution of human auditory evoked potentials. I. Evaluation of reference electrode sites. Electroencephalogr. Clin. Neurophysiol. 54, 15–24.
Woo, C.-W., Chang, L.J., Lindquist, M.A., Wager, T.D., 2017. Building better biomarkers: brain models in translational neuroimaging. Nat. Neurosci. 20, 365–377.
Yao, D., 2001. A method to standardize a reference of scalp EEG recordings to a point at infinity. Physiol. Meas. 22, 693–711.
Yao, D., Wang, L., Oostenveld, R., Nielsen, K.D., Arendt-Nielsen, L., Chen, A.C.N., 2005. A comparative study of different references for EEG spectral mapping: the issue of the neutral reference and the use of the infinity reference. Physiol. Meas. 26, 173–184.
Yu, X., Zhang, J., Xie, D., Wang, J., Zhang, C., 2009. Relationship between scalp potential and autonomic nervous activity during a mental arithmetic task. Auton. Neurosci. 146, 81–86.